İSTANBUL TECHNICAL UNIVERSITY ★ INSTITUTE OF SCIENCE AND TECHNOLOGY

DEPOSITION OF COPPER THIN FILMS ON PLASMA TREATED POLYIMIDE SURFACES

M.Sc. Thesis by
Meryem Öznur PEHLİVANER

Department : Advanced Technologies

Programme : Material Science and Engineering

JUNE 2011

İSTANBUL TECHNICAL UNIVERSITY ★ INSTITUTE OF SCIENCE AND TECHNOLOGY

DEPOSITION OF COPPER THIN FILMS ON PLASMA TREATED POLYIMIDE SURFACES

M.Sc. Thesis by
Meryem Öznur PEHLİVANER
(521091025)

Date of submission :	**06 May 2011**
Date of defence examination:	**07 June 2011**

Supervisor (Chairman) :	**Assist. Prof. Dr. Hüseyin KIZIL (ITU)**
Members of the Examining Committee :	**Prof. Dr. Servet TİMUR (ITU)** **Prof. Dr. Sezai SARAÇ (ITU)**

JUNE 2011

İSTANBUL TEKNİK ÜNİVERSİTESİ ★ FEN BİLİMLERİ ENSTİTÜSÜ

PLAZMA İŞLEMİ UYGULANMIŞ POLYİMİDE YÜZEYLERİNE BAKIR KAPLANMASI

YÜKSEK LİSANS TEZİ
Meryem Öznur PEHLİVANER
(521091025)

Tezin Enstitüye Verildiği Tarih : 06 Mayıs 2011
Tezin Savunulduğu Tarih : 07 Haziran 2011

Tez Danışmanı : Yrd. Doç. Dr. Hüseyin KIZIL (İTÜ)
Diğer Jüri Üyeleri : Prof. Dr. Servet TİMUR (İTÜ)
Prof. Dr. Sezai SARAÇ (İTÜ)

HAZİRAN 2011

FOREWORD

I would like to express my deep appreciation and thanks for my advisor, Assis. Prof. Dr. Hüseyin KIZIL, for giving me the opportunity to work on this project.

I also would like to express my sincere thanks to Assoc. Prof. Dr. Levent TRABZON for his academic advice and support.

I would like to express my gratitudes to Prof. Dr. Servet TİMUR for his support, guidance and suggestions.

My deepest gratitude to Sebahattin GÜVENDİK and Vural KARA for working with me until midnight and making a nice atmopshere at the work. This thesis could not have been completed without their invaluable support, advice and encouragement.

I would also like to thank my friends; M. Ragıp ABDULLAHOĞLU, Aykut YILMAZ, Berat DOĞAN and Emine BAKAN for their support and my lab mates whom I enjoyed my research and study at ITU-MEMS.

Finally, it's my deepest pride to thank here my family for never-ending belief throughout my life.

June 2011 Meryem Öznur Pehlivaner

Textile Engineering

TABLE OF CONTENTS

Page

TABLE OF CONTENTS ..... **vii**
ABBREVIATIONS ..... **ix**
LIST OF TABLES ..... **xi**
LIST OF FIGURES ..... **xiii**
SUMMARY ..... **xv**
ÖZET ..... **xvii**
1. INTRODUCTION **1**
2. LITERATURE **3**
  2.1 Plasma modification 3
  2.2 Magnetron Sputtering 8
  2.3 Electroplating 9
    2.3.1 Electroplating mechanism 10
    2.3.2 Electroplating parameters 11
    2.3.3 Two step electroplating 13
    2.3.4 Pulse plating 14
3. EXPERIMENTS AND RESULTS **19**
  3.1 Plasma Process 19
    3.1.1 Sample preparation 19
    3.1.2 Plasma modification 19
    3.1.3 Contact angle measurements 21
    3.1.4 AFM analysis 23
    3.1.5 FTIR analysis 26
  3.2 Magnetron Sputtering 27
    3.2.1 Deposition of Ti and Cu seed layer on the polyimide substrate 28
  3.3 Magnetron Sputtering 30
    3.3.1 Effect of current density 32
    3.3.2 Effect of pulse waveforms 35
4. CONCLUSION AND RECOMMENDATIONS **39**
REFERENCES **41**
CURRICULUM VITAE **45**

ABBREVIATIONS

AFM **:** Atomic force microscopy
FTIR **:** Fourier transform infrared spectroscopy
ICP **:** Inductively coupled plasma
MEMS **:** Micro-electro-mechanical-systems
PI **:** Polyimide
PVD **:** Physical vapour deposition
RMS **:** Root mean square of roughness
SEM **:** Scanning electron microscopy

LIST OF TABLES

Page

Table 3.1: The settings for the plasma modification on PI films. 20
Table 3.2: The settings for Ti deposition on PI films. 29
Table 3.3: The settings for Cu deposition on PI films. 30
Table 3.4: The settings for the copper electroplating on Cu/Ti/PI films.................. 31
Table 3.5: The average roughness of the copper films as a function of the current density. 32

LIST OF FIGURES

Page

Figure 2.1 : Two dimensional AFM images of (a) unmodified, (b) 0.5 min, (c) 1 min, (d) 3 min of oxygen plasma modified Kapton E [5]....................... 4
Figure 2.2 : Two dimensional AFM images of (a) unmodified, (b) 0.5 min, (c) 1 min, (d) 3 min of oxygen plasma modified Upilex S [5]........................ 4
Figure 2.3 : Surface energies of oxygen plasma-modified polyimide substrates as a function of plasma modification duration [5]. 5
Figure 2.4 : Proportion of chemical bonds for un-modified and oxygen plasma modified (a) Kapton E and (b) Upilex S as a function of plasma modification duration [5]. 5
Figure 2.5 : 4 x4μm^2 AFM image of the oxygen plasma treated PI surfaces with substrate bias power of (a) untreated, (b) 0W, (c) 60W, (d) 125W [6] . 6
Figure 2.6 : Contact angles and RMS roughness as a function of bottom power [6]. 7
Figure 2.7 : Wide scan spectra of the untreated (a) and oxygen plasma treated PI films as a function of substrate bias power; (b) 0W, (c) 60W, (d) 125W [6].. 7
Figure 2.8 : Peel strength as a function of seed layer thickness [17]. 8
Figure 2.9 : Relationship between chemical bonding and peel strength as a function of the seed layer thickness [17]... 9
Figure 2.10 : Schematic represantation of the electroplating system [20]................ 11
Figure 2.11 : Deposition rate and surface morphology as a function of current density hematic represantation of the electroplating system [19]. 11
Figure 2.12 : Film thickness as a function of electrode distance [19]. 12
Figure 2.13 : SEM images as a function of electrode distance; (a) 1 cm, (b) 2cm, (c) 3cm [19].. 13
Figure 2.14 : Proposed model for smaller copper grain growth during normal pulse plating [24]. 14
Figure 2.15 : AFM images of a pulsed reverse copper plating [21]. 15
Figure 2.16 : Different combinations of pulse wave forms [23].............................. 16
Figure 2.17 : SEM images of line trenches and via holes as a function of different pulse waveform; (a) 3ms on + 0.5 ms off, (b) 6ms on + 2 ms off, (c) 8ms on + 1 ms off, (d) 9.9 ms on + 2.5 ms off [24]. 17
Figure 3.1 : Inductively coupled plasma.. 20
Figure 3.2 : Plasma creation.. 20
Figure 3.3 : Contact angle values of argon plasma treated Kapton HN and Kapton TABE films as a function of duration.. 21
Figure 3.4 : Contact angle values of oxygen plasma treated Kapton HN and Kapton TABE films as a function of duration.. 22
Figure 3.5 : Contact angle images of argon plasma treated Kapton HN films as a function of a duration (a) unmodified, (b) 1 min, (c) 3 min, (d) 5 min. 22

Figure 3.6 : Contact angle images of argon plasma treated Kapton TABE films as a function of a duration (a) unmodified, (b) 1 min, (c) 3 min, (d) 5 min. 22
Figure 3.7 : Contact angle images of oxygen plasma treated Kapton HN films as a function of a duration (a) unmodified, (b) 1 min, (c) 3 min, (d) 5 min. 23
Figure 3.8 : Contact angle images of oxygen plasma treated Kapton TABE films as a function of a duration (a) unmodified, (b) 1 min, (c) 3 min, (d) 5 min. 23
Figure 3.9 : 4.0 x 4.0 μm^2 AFM image of argon plasma treated Kapton TABE surfaces as a function of duration; (a) untreated, (b) 3 min, (c) 5 min. 24
Figure 3.10 : 4.0 x 4.0 μm^2 AFM image of oxygen plasma treated Kapton TABE surfaces as a function of duration; (a) untreated, (b) 1 min, (c) 3 min, (d) 5 min. 25
Figure 3.11 : Relationship between contact angle and RMS roughness of oxygen plasma treated Kapton TABE films as a function of duration. 25
Figure 3.12 : Relationship between contact angle and RMS roughness of argon plasma treated Kapton TABE films as a function of duration. 26
Figure 3.13 : FTIR spectra of argon plasma treated Kapton TABE films as a function of duration (a) 5 min (b) 1 min (c) 0 min (d) 3 min 27
Figure 3.14 : Physical vapor deposition system 28
Figure 3.15 : Sputtering yields data for metals [31] 30
Figure 3.16 : The experimental setup. 31
Figure 3.17 : SEM micrographs of electroplated copper at a mean current density of 4mA/cm^{-2} 32
Figure 3.18 : SEM micrographs of electroplated copper at a mean current density of 8 mA/cm^{-2} 33
Figure 3.19 : SEM micrographs of electroplated copper at mean current density of 12 mA/cm^{-2} 33
Figure 3.20 : Conc SEM micrographs of the electroplated copper at a mean current density of 16 mA/cm^{-2} 34
Figure 3.21 : SEM micrographs of the electrplated copper at a mean current density of 20 mA/cm^{-2} 34
Figure 3.22 : SEM micrograph of the electroplated copper at pulse waveform of 60 ms on + 40 ms off and a current density of 2 mA/cm^{-2} 36
Figure 3.23 : SEM micrograph of the electroplated copper at pulse waveform of 70 ms on + 30 ms off and a cuurent density of 4 mA/cm^{-2} 36
Figure 3.24 : SEM micrograph of the electroplated copper at 80 ms on + 20 ms off and a current density of 6 mA/cm^{-2} 37
Figure 3.25 : SEM micrograph of the electroplated copper at 90 ms on + 10 ms off and a current density of 8 mA/cm^{-2} 37

DEPOSITION OF COPPER THIN FILMS ON PLASMATREATED POLYIMIDE SURFACES

SUMMARY

Flexible electronics and micro-electro-mechanical devices have drawn much attention because they have wider application field, provides low cost and ease of fabrication when we compare to the silicon based electronic devices. For fabrication flexible electronics and MEMS devices, metals must be deposited on flexible substrates. In this study, polyimide was selected as a flexible substrate because of its desirable properties; good mechanical strength, high temperature resistance, good dimensional stabilities and low dielectric constant. The adhesion strength between metal and polymer is a critical issue. To overcome this problem, plasma surface modifications were used on polyimide surface by inductively coupled plasma treatment system. The results of contact angle measurements and atomic force microscopy (AFM) show a large increase in surface roughness with increasing duration and complete wetting after argon and oxygen plasma treatment. Analysis of chemical composition by Fourier transform infrared spectroscopy (FTIR) shows an increase in carbon-oxygen functional groups and the concentration of oxygen on the surfaces for argon plasma treated polyimide. To attain further improvement on adhesion between polyimide and metal, thin metal adhesion promoting layer (120 nm) was used before sputtering copper seed layer (200 nm). At last step, pulse reverse plating technique was used for attaining blanket layer on polyimide films. The electroplating experiments show that the smooth surface morphology is obtained at a mean current density of 8 mA/cm^2 and 90 ms on period, 10 ms off period. SEM micrographs show that the balanced on and off periods give the smooth, uniform surface morphology. 90 ms on period and 10 ms off period were selected as optimum pulse waveforms. By this method, fine metallization with few micrometers was observed.

PLAZMA İŞLEMİ UYGULANMIŞ POLYİMİDE YÜZEYLERİNE BAKIR KAPLANMASI

ÖZET

Silisyum temelli elektronik cihazlar ile karşılaştırıldığında, daha geniş uygulama alanına sahip olmaları, düşük maliyetli ve kolay üretim imkanı sağlamalarıyla esnek elektronik cihazlar ve mikro-elektro-mekanik-sistemler (MEMS) dikkatleri üzerlerine çekmektedirler. Esnek elektronik cihazların ve MEMS donanımlarının üretimi için, esnek altlık malzeme üzerine metal kaplanması gerekmektedir. Bu çalışmada, polyimide, iyi mekanik dayanım, yüksek sıcaklık dayanımı, iyi boyutsal kararlılık ve düşük dielektrik katsayısı gibi cazip özellikleri sebebiyle, esnek altlık malzeme olarak seçilmiştir. Metal ve polimer arasındaki adezyon kuvveti hassas bir konudur. Bu problemi aşmak için, etkileşik çiftlenmiş plazma yöntemiyle polyimide yüzeyleri üzerinde plazma yüzey modifikasyonları uygulanmıştır. Argon ve oksijen plazma işlemi sonunda, ölçülen kontak açı ve atomsal kuvvet mikroskopisi (AFM) sonuçları artan süreyle birlikte yüzey pürüzlülüğünde büyük bir artma ve polyimide yüzeylerinde ise tam ıslanma olduğunu göstermektedir. Fourier dönüşümlü kızılötesi spektroskopisi (FTIR) ile yapılan kimyasal yapı analizi ise argon plazma işlemi sonrasında yüzeyde karbon-oksijen fonksiyonel gruplarında ve yüzeydeki oksijen miktarında artma olduğunu göstermektedir. Sıçratma yöntemiyle 200 nm kalınlığında çekirdek bakır tabakasının kaplanmasından önce metal ve polyimide arasındaki adezyonu daha da güçlendirmek için 120 nm adezyonu artırıcı ince bir metal tabaka kullanılmıştır. Son aşamada ise, pulse-reverse kaplama tekniği polyimide yüzeyler üzerinde blanket bakır tabakasının elde edilmesinde kullanılmıştır. Ortalama akım yoğunluğu 8 mA/cm^2, açık periyot 90 ms, kapalı periyot 10 ms iken düzgün, pürüzsüz yüzeyler elde edilmiştir. SEM mikrografları göstermektedir ki dengeli pulse dalga formları düzgün ve uniform yüzey morfolojisi vermektedir. 90 ms açık periyot, 10 ms kapalı periyot optimum dalga formları olarak belirlenmiştir. Bu yöntemle birkaç mikrometre kalınlığında kaliteli bir metal kaplama gözlemlenmiştir.

1. INTRODUCTION

Polymers have long been one of the most commonly used material in many industries. There are many applications such as food packaging, durable fibres, resins for photo resists, advanced composites, biopolymers [1]. Electronic industry is one of the application areas of polymers, and among them, polyimide is the most used polymer in electronic industry due to its desirable properties; good mechanical strength, high temperature resistance, good dimensional stabilities and low dielectric constant.

Polyimide is the material of choice as a substrate for flexible electronics and Micro-Electro-Mechanical-Systems (MEMS). Silicon based MEMS are not appropriate for non-rigid or non-planar surfaces while flexible substrates can bend and twist so as to absorb the stress. Also, flexible substrates provide low-cost and ease of fabrication.

Many studies can be found in the literature in the field of flexible electronics and MEMS devices including flexible thin films transistor, flexible printed circuit boards, organic light emitting devices, photovoltaic devices, flexible MEMS systems, liquid crystal displays and flexible flat panels [2]. Flexible tactile sensors, which can be used as the fingertips or hands of humanoid robots in the area of medicine, robotics and industrial automation, are among the most studied areas in flexible MEMS [3].

There are four basic fabrication steps; plasma treatment for better adhesion between metal and polymer, adhesion promoting metal and seed layer deposition for attaining conductive layer on polyimide films, photolithography for patterning of metals and electroplating. In this thesis, plasma treatment, seed layer metal deposition and Cu electroplating were performed on polyimide films. Patterning the polyimide substrate by photolithography will be investigated in another study with the guidance of this current study.

2. LITERATURE

2.1 Plasma modification

Adhesion between polyimide and copper is a critical issue in the area of electronic packaging devices [4]. To improve the strentgh of the boundary layer between polyimide and metal, different types of treatments such as plasma [2,5-13], ion beam [14,15], or chemical treatment [16] are used. Inagaki et al. stated that different types of plasma gases such as Ar, N_2, NO, NO_2, O_2, CO, CO_2, atmospheric can be used as a plasma gas for treatment [16]. Lin et. al. investigated different plasma gases; oxygen, nitrogen, argon effects on polyimide films Kapton E and Upilex S [10,7,5]. The experiments are performed at 200W of power, 60mTorr of chamber pressure, 10 sccm of gas flow rate. Also, the experiments are carried out in three different duration intervals; 0, 1, 3 min. The optimum results are obtained at 3 min. treated films for Kapton E and Upilex S for oxygen plasma. After oxygen treatment of the surfaces, the peel strengths enhance from 1.2 g/mm and 0.7 g/mm for sputtured copper thin films on Kapton E and Upilex S to 262.2 g/mm and 195.5 g/mm for sputtered copper films on oxygen plasma treated Kapton E and Upilex S for a duration of 3 min. Plasma modification induces the mechanical, chemical and physical changes on polyimide substrates. As seen in the Fig. 2.1 and Fig. 2.2, the surfaces of Kapton E and Upilex S become roughened by oxygen plasma treatment. The most roughened and crosslinkid surfaces of Kapton E and Upilex S are observed at duration of 3 min. Plasma surface modification has an enormous effect on surface energy on PI films. Fig. 2.3 shows the surface energy of Kapton E and Upilex S as a function of duration. Nano scale surface roughness may decreases the contact angle by generating hydrophilic functional groups on surface or increases the contact angle by generating hydrophobic functional groups on surface [12]. When we compare to the AFM results, we can say that the increased surface roughness induces the increase in surface energy. The maximum surface energy is observed at duration of 3 min.

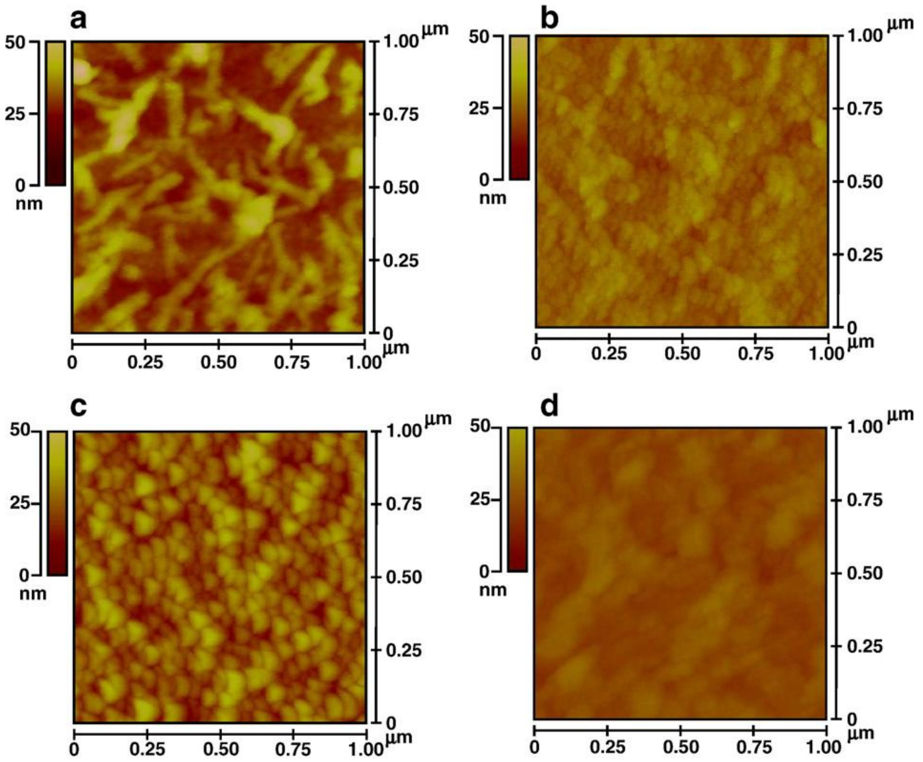
a
b
c
d
50
25
0
nm
1.00 µm
0.75
0.50
0.25
0
0
0.25
0.50
0.75
1.00 µm

Figure 2.1 : Two dimensional AFM images of (a) unmodified, (b) 0.5 min, (c) 1 min, (d) 3 min of oxygen plasma modified Kapton E [5].

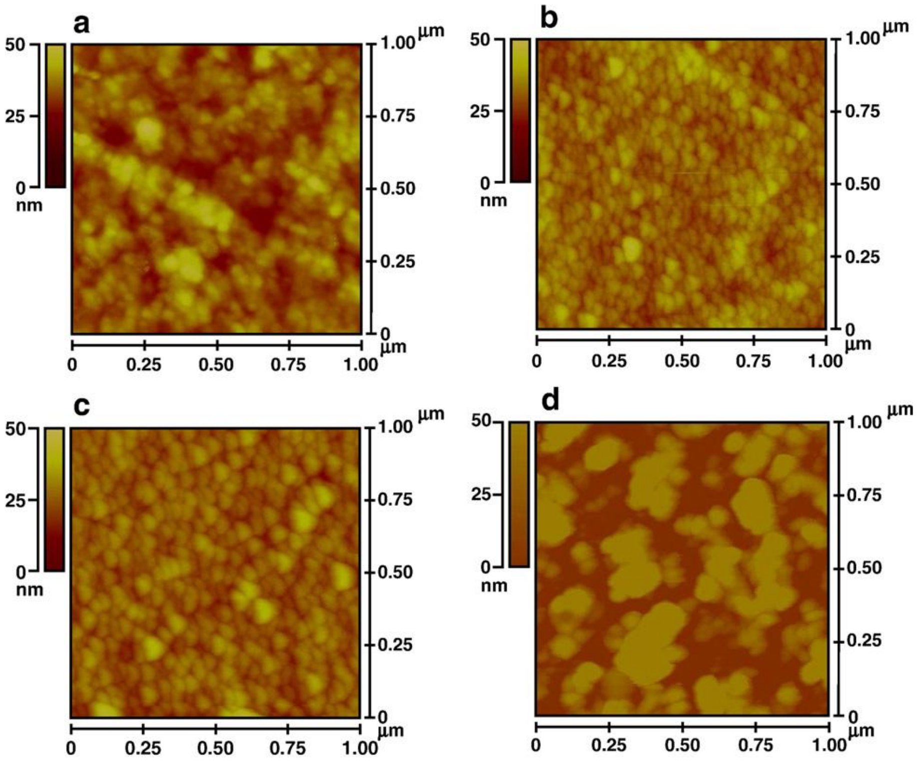
a
b
c
d
50
25
0
nm
1.00 µm
0.75
0.50
0.25
0
0
0.25
0.50
0.75
1.00 µm

Figure 2.2 : Two dimensional AFM images of (a) unmodified, (b) 0.5 min, (c) 1 min, (d) 3 min of oxygen plasma modified Upilex S [5].

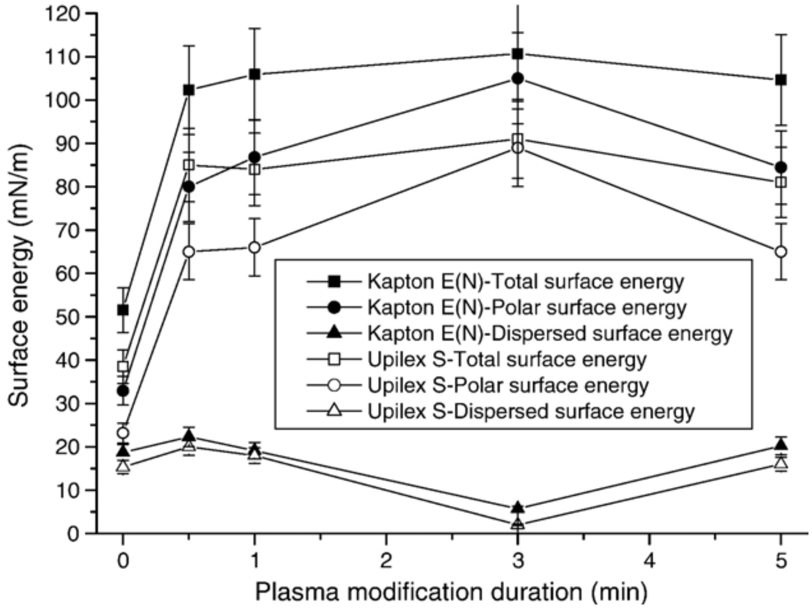

Figure 2.3 : Surface energies of oxygen plasma-modified polyimide substrates as a function of plasma modification duration [5].

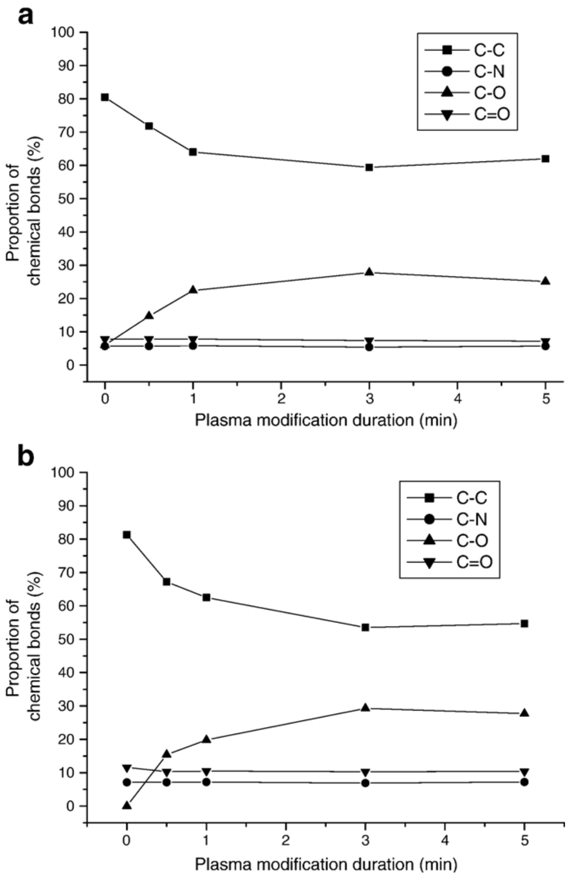

Figure 2.4 : Proportion of chemical bonds for un-modified and oxygen plasma modified (a) Kapton E and (b) Upilex S as a function of plasma modification duration [5].

Fig 2.4 shows that the proportion of the chemical bonds as a function of duration. It is observed that oxygen plasma improves the surface energies of polyimide substrates by increasing oxygen surface concentration and C-O bond proportion.

Two different studies were performed by the same group. The experimental conditions are the same except the plasma gases, argon and nitrogen. After argon treatment of the surfaces, the peel strengths enhance from 1.2 g/mm and 0.7 g/mm for sputtered copper thin films on Kapton E and Upilex S to 110.3 g/mm and 98 g/mm for sputtered copper films on argon plasma treated Kapton E and Upilex S for a duration of 1 min [10]. Also nitrogen plasma enhances the peel strentgh from 1.2 g/mm and 0.7 g/mm sputtered copper thin films on Kapton E and Upilex S to 152.2 g/mm and 140.1 g/mm for sputtered copper films on argon plasma treated Kapton E and Upilex S for a duration of 1 min [7]. The significant difference between the previous study is stated by this group that an increase in C-O, C=O, C-N for argon and an increase in C-O, improves the adhesive strength between polyimide and copper. The second effective parameter in plasma process is plasma power. Kim et. al. [6] stated that substrate bias power controls the bombardment energy of the ions in the ICP system. Excessive substrate bias power density induces the excessive chain scission on polyimide surface and leads to the weak boundary layer between polymer and metal so they selected the low substrate bias power density. The oxygen plasma treatments are performed at the top power of 40W and the bottom power of 0, 60, 125W. According to the results, the maximum peel strength value of 126 gf/mm is observed at bottom power of 125W.

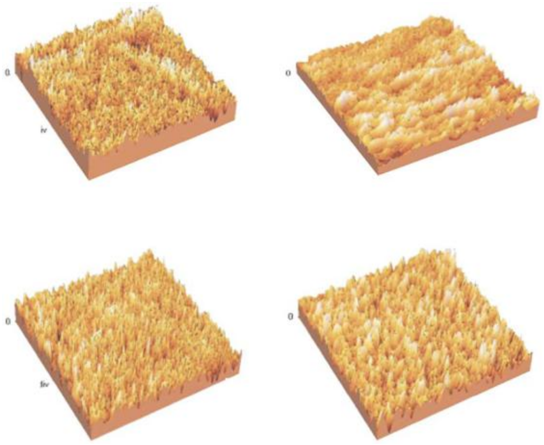

Figure 2.5 : 4 x4μm^2 AFM image of the oxygen plasma treated PI surfaces with substrate bias power of (a) untreated, (b) 0W, (c) 60W, (d) 125W [6] .

As seen in Fig. 2.5, the increased substrate bias power increases the surface roughness by increased bombardment energy of oxygen ions. The most cross linked surface is observed at substrate bias power of 125W. Fig. 2.6 shows the correlation between the contact angle and RMS roughness. The results shows that the large increase in the surface roughness provides complete wetting condition and improves the surface roughness.

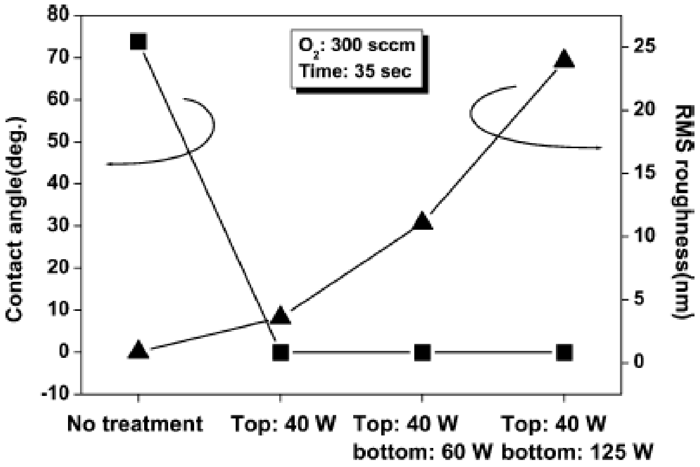

Figure 2.6 : Contact angles and RMS roughness as a function of bottom power [6].

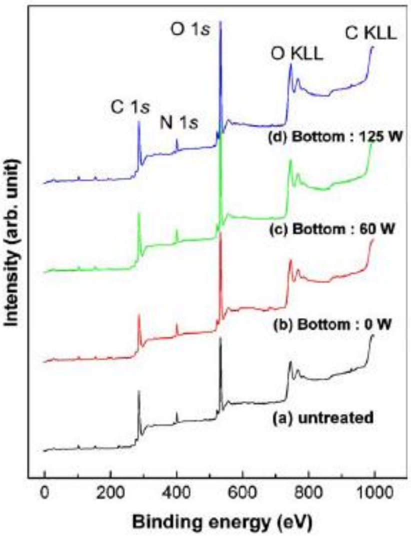

Figure 2.7 : Wide scan spectra of the untreated (a) and oxygen plasma treated PI films as a function of substrate bias power; (b) 0W, (c) 60W, (d) 125W [6].

When we look at the XPS results as a function of bottom power in Fig. 2.7, we realized that the intensities of the C 1s and O 1s spectra increase by increased bottom power. As a result of oxygen plasma modification, new functional groups; C-O and C=O are observed on the surface of the polyimide film.

2.2 Magnetron Sputtering

To improve the adhesive strength between polyimide and copper, the adhesion promoting layer; Cr, Ni, NiCr, Ti, ITO is used after plasma treatment [17]. The adhesion strength is determined by the chemical bonding in polymer surfaces and metal-polymer interfaces. Kim et. al. selected 50 nm thin Cr layer as an adhesion promoter prior to the copper sputtering, Ni layer is deposited by magnetron sputtering at argon flow of 20 sccm, chamber pressure of 2mTorr, power of 100W. Copper deposition parameters are same [6]. Noh et. al. [17] investigated the effect of seed layer thickness on the adhesion strentgh of Cu/Ni-Cr/polyimide films for flexible printed circuits. After argon ion treatment on polyimide surface, Ni-Cr (Ni:Cr=95:5 ratio) layers with thickness of 100 Å, 200 Å, 300Å are deposited at flow rate of 120 sccm, power of 600W,800W,1200W by magnetron sputtering prior to copper electroplating. As seen in Fig. 2.8, the peel strength increases with the increasing seed layer thickness. Furthermore, after peel test, the surface roughness of the fracture samples are measured by AFM. The RMS roughness increases with the increasing seed layer thickness so we can say that boundary layer becomes stronger with increasing seed layer thickness.

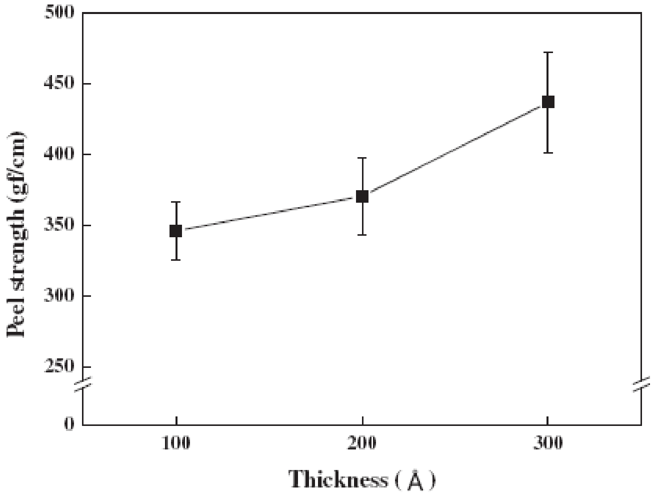

Figure 2.8 : Peel strength as a function of seed layer thickness [17].

Fig. 2.9 shows that the relationship between the peel strentgh and chemical bonding ratio as a function of seed layer thickness. It is estimated that the reaarrangement of the C-N bonding during Ni-Cr deposition causes the increase in C-O bonding. As a result, the formation of Cr-O-C bonding increases the adhesion strentgh.

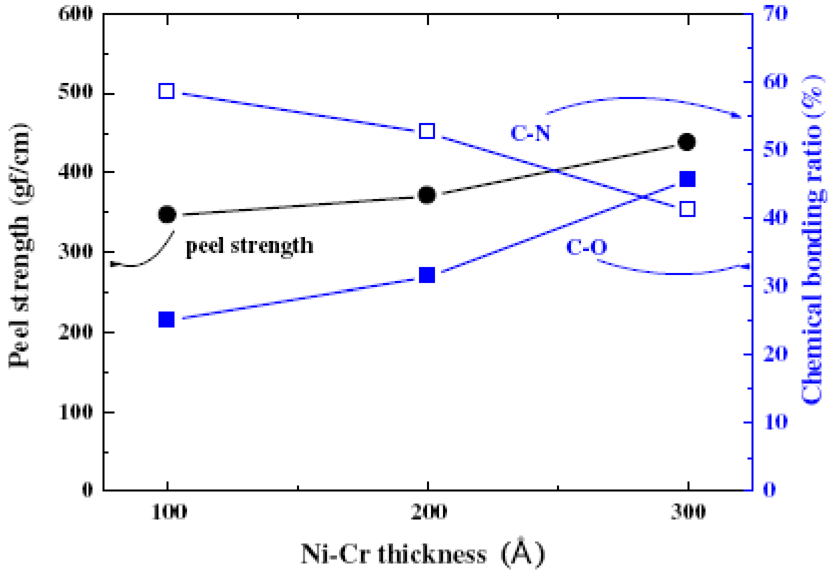

Figure 2.9 : Relationship between chemical bonding and peel strength as a function of the seed layer thickness [17].

2.3 Electroplating

Electroplating is a process which metal ions migrate from the anode to the cathode through an electrolyte and deposit on the cathode surface by an external electric current. Various materials like metals, conductive polymers, metal alloys and some semiconductors can be deposited by the electroplating method. There are seventeen metals which can be used for this process. But some of them is appropriate for micro-electrodeposition. Copper is mostly used one. Because it has low resistivity (1.6730 x 10^{-6} Ω/cm), excellent gap fill capability and higher allowed current density, it can be deposited directly on a wafer or non conductive material with a thin metal seed layer [8,18].

The copper films can be deposited using various techniques such as PVD, CVD and electroplating. However the CVD method cannot be used in the manufacturing applications because of high cost, great film stress and low deposition speed [19] .

PVD methods such as sputtering, e-beam evaporation and thermal evaporation cause some problems during filling trenches holes because of shadow effect. But electroplating technique has many advantages over PVD and CVD techniques:

- low temperature process. (for copper at room temperature)
- quick process, it takes only few seconds.
- no clean room needed
- low operating cost
- precise control
- great reliability for high aspect ratio structures

Also the deposited material's properties such as texture, grain size, crystallographic structure and composition can be easily controlled by plating parameters such as deposition temperature, pH, current density, bath composition and agitation.

2.3.1 Electroplating mechanism

The sample and copper immersed in the bath. The sample and copper are connected to the cathode and the anode terminals respectively. When the sufficient potential is provided between anode and cathode, electrons move from anode to cathode. Cathode and anode reactions occur as follows:

Cathode reaction:

$$Cu^{+2} + 2e^{-} \rightarrow Cu \qquad \textbf{(2.1)}$$

Anode reaction:

$$Cu \rightarrow Cu^{+2} + 2e^{-} \qquad \textbf{(2.2)}$$

As seen in Fig. 2.10, electroplating setup consists of:

- an electrically conductive substrate such as wafer or non-conductive substrate like polymers. If a non-conductive substrate will be used, a thin metal film must be deposited to obtain conducting surface on the substrate by sputtering.
- an electrolyte solution
- current or voltage source

- a counter electrode
- a reference electrode.

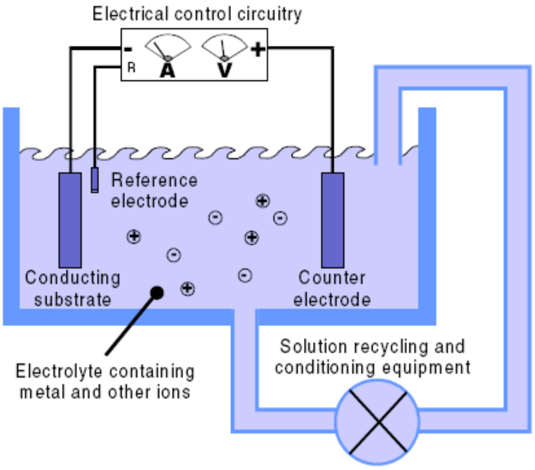
Electrical control circuitry
-
+
R
A
V
Reference electrode
Conducting substrate
Counter electrode
Electrolyte containing metal and other ions
Solution recycling and conditioning equipment

Figure 2.10 : Schematic represantation of the electroplating system [20].

2.3.2 Electroplating parameters

Current density can be obtained by dividing the deposition current to the deposition area. Studies have shown that the current density has an enormous effect on the deposition rate, the resistivity and the surface morphology [19,21]. Film resistivity can be obtained by calculation of the sheet resistance and the film thickness. The resistivity of the film changes suddenly at high current densities because small and rougher grain increased the resistivity of the film sharply.

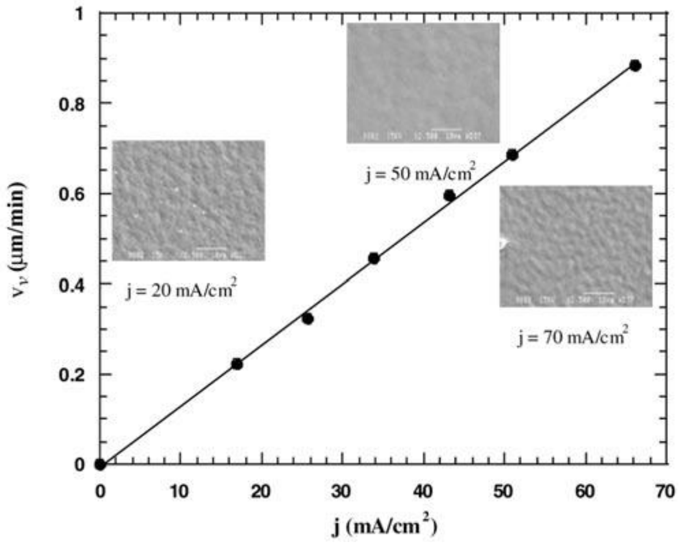

Figure 2.11 : Deposition rate and surface morphology as a function of current density hematic represantation of the electroplating system [19].

The proper current density should be determined according to the appropriate surface morphology and resistivity. Fig. 2.11 shows that grain size decreased with the increasing current density. Smoother surface is obtained at 50 mA/cm^2. Temperature has an enormous effect on electroplating. Studies have shown that the films plated with high current densities have the small surface irregularities with increasing bath temperature than the films plated with low current densities [22]. The most favoured temperature for copper electroplating in acid copper solutions is 25 °C - 30 °C.

During electroplating, the concentration of ions will reduce around the cathode. Agitation is necessary for elimination of low concentration areas. Also agitation is a useful method which is used to remove hydrogen bubbles from cathode surface [23].

There are four types of copper plating solutions: cyanide, pyrophosphate, fluoborate and acid copper solutions. Cyanide solutions have waste treatment problems because of their toxicity. So noncyanide solutions can be used instead of cyanide solutions. Fluoborate solutions are used at high current densities. But acid copper sulphate solutions have many advantages such as easy to control, quick to prepare and low cost. Acid copper sulphate solution is the most preferred one. Acid copper sulphate solutions consist of $CuSO_4$, H_2SO_4 and additives.

Park et. al. investigated the electrode distance effect for copper electroplating on Si wafer. The experiments are performed for 3 min with current density from 2.4 A/dm^2 to 3.2 A/dm^2 and electrode distance from 1 cm to 4cm. As seen in Fig. 2.12, film thickness increases with the reduced electrode distance. Also, Fig. 2.13 shows the SEM images as a function of a electrode distance.

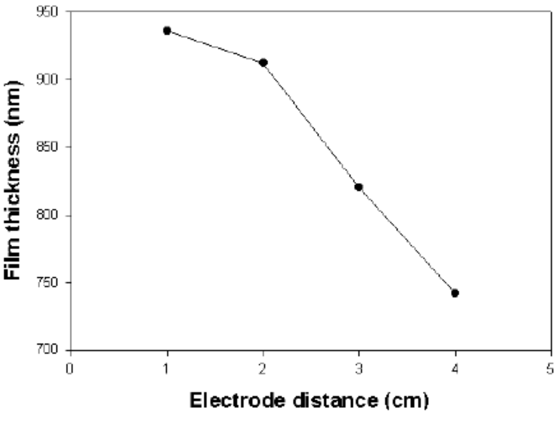

Figure 2.12 : Film thickness as a function of electrode distance [19].

The images show that the films plated with large electrode distance have the bad roughness and the lower deposition rate than the films plated with small electrode distance. But there was no difference between in grain sizes and shapes between different electrode distances [19].

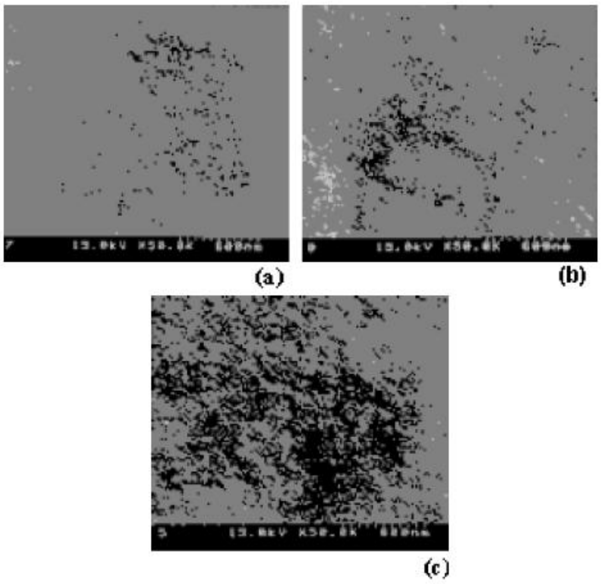

Figure 2.13 : SEM images as a function of electrode distance; (a) 1 cm, (b) 2cm, (c) 3cm [19].

2.3.3 Two step electroplating

Two step electroplating technique can be preferred in order to solve adhesion problems obtain uniform and faster plating. Seah et al. [24] have studied on filling of the sub-0.25 µm line trenches and contact vias by two step electroplating. In the first step, a low current density of 0.05 A/m^2 and a short deposition time of 2s were applied for copper electrodeposition. By this way, the small copper crystallites nucleate the entire surface regularly. In the second step, a high current density of 0.15 A/m^2 and a high deposition time of 30 s were applied due to faster deposition. The deposition time was 70 s at normal condition for complete filling. Fujita et al. [25] have studied different two step electroplating technique. In this method, an annealing process replaced between the first and second electroplating and occurred at 250 C° for 30 min and 3mTorr vacuum condition. They achieved gold electroplating on silicon surface for MEMS applications without seed layer.

2.3.4 Pulse plating

Pulse plating is an alternative technique instead of DC plating. Peak current density, the cathodic duration (on time) and the presence of reversed current (off time) parameters can be controlled in pulse plating but in DC plating, there is only one parameter; current [23]. The films plated with DC plating have the larger grain size than the films plated with pulse plating because there is only one nucleation step in DC plating, whereas pulse plating involves on and off periods in the total pulse cycle. New nucleation occurs at every on period of pulse cycle. Fig. 2.14 indicates the grain growth in pulse plating. In this study, TaN is used as a seed layer for copper electroplating on Si wafer.

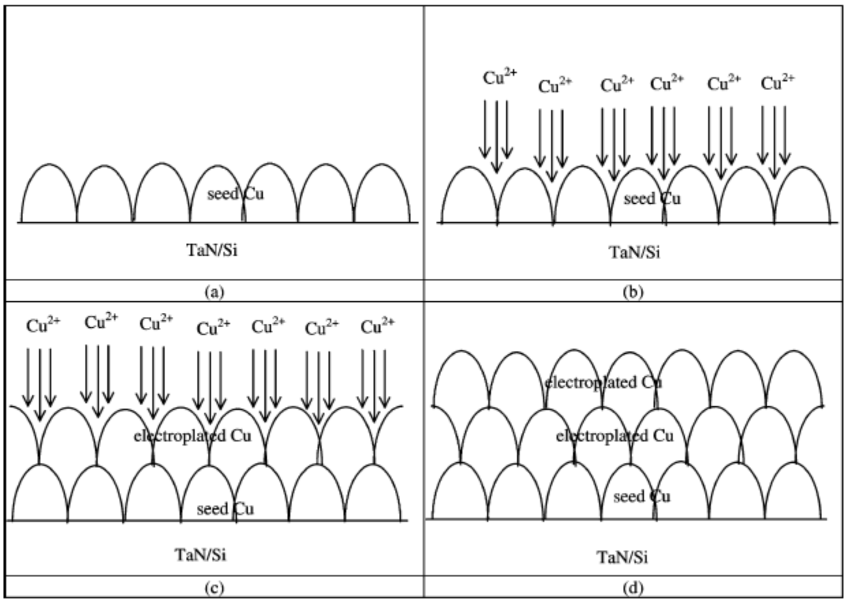

Figure 2.14 : Proposed model for smaller copper grain growth during normal pulse plating [24].

Also new grains grow continually with increasing deposition time but a lower rate than DC plating and align along the new grain boundaries of electroplated copper. As seen in Fig. 2.15, fine grains of size less than or equal 0.1 μm are produced in pulse plating. Seah et al. [24] reported that there is no important difference between the grain size and growth pattern of copper films plated with different current densities in pulse plating. Also negatively charged layer is formed around the cathode during electroplating process. In DC plating, this layer charges with a definite thickness blocks the ions from the reach the part. But in pulse plating, when current is not applied at T_{OFF}, this layer discharges. By this way, the ions pass through the layer and reach the part easily. Furthermore, high current density zones involve more consumed of ions than low current density zones in the bath. In pulse plating, during off time, ions move to the consumed zones in the bath and distribute equally for deposition [26]. Zinsou [27] has achieved to obtain uniform, void free and conformal films on patterned Si wafer with seed layer using the forward current density of 13 mA/cm^2 at 15 ms and the reverse current density of -27 mA/cm^2 at 1 ms. Also total cycle was completed at 20 min.

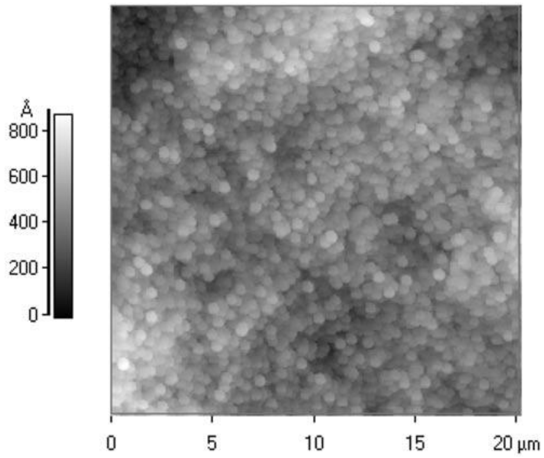

Figure 2.15 : AFM images of a pulsed reverse copper plating [21].

Fig. 2.16 shows the different pulse wave forms for electroplating such as; pulse super imposed pulse, duplex pulse, pulsed pulse, pulse on pulse, pulse reverse, pulse reverse with off tine, pulsed pulse reverse in pulse plating. Quemper et al. have investigated the effects of different pulse wave forms with ranging from 3ms on + 0.5 ms off to 9.9 ms on + 2.5 ms off on copper deposition through photo resist molds [21]. As seen in Fig. 2.17, too high on period induces the copper growth fast and leading to the pinch off the via.

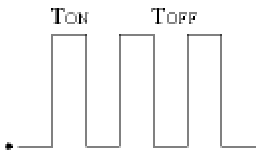

PULSE

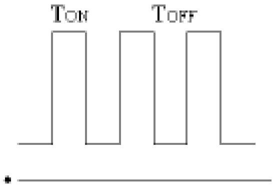

SUPER IMPOSED PULSE

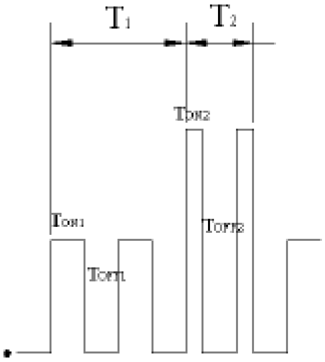
T1
T2
TON2
TON1
TOFF2
TOFF1

DUPLEX PULSE

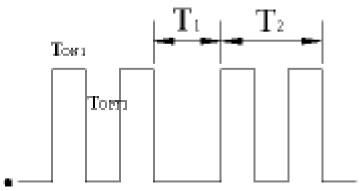
T1
T2
TON1
TOFF1

PULSED PULSE

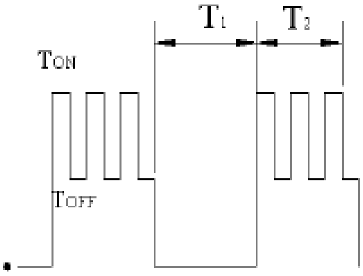
T1
T2
TON
TOFF

PULSE ON PULSE

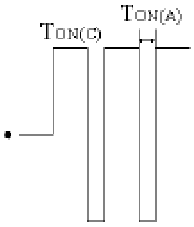

PULSE REVERSE

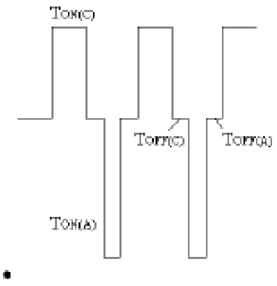
TON(C)
TOFF(C)
TOFF(A)
TON(A)

PULSE REVERSE
WITH OFF TIME

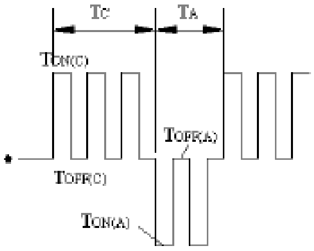
TC
TA
TON(C)
TOFF(A)
TOFF(C)
TON(A)

PULSED PULSE REVERSE

Figure 2.16 : Different combinations of pulse wave forms [23].

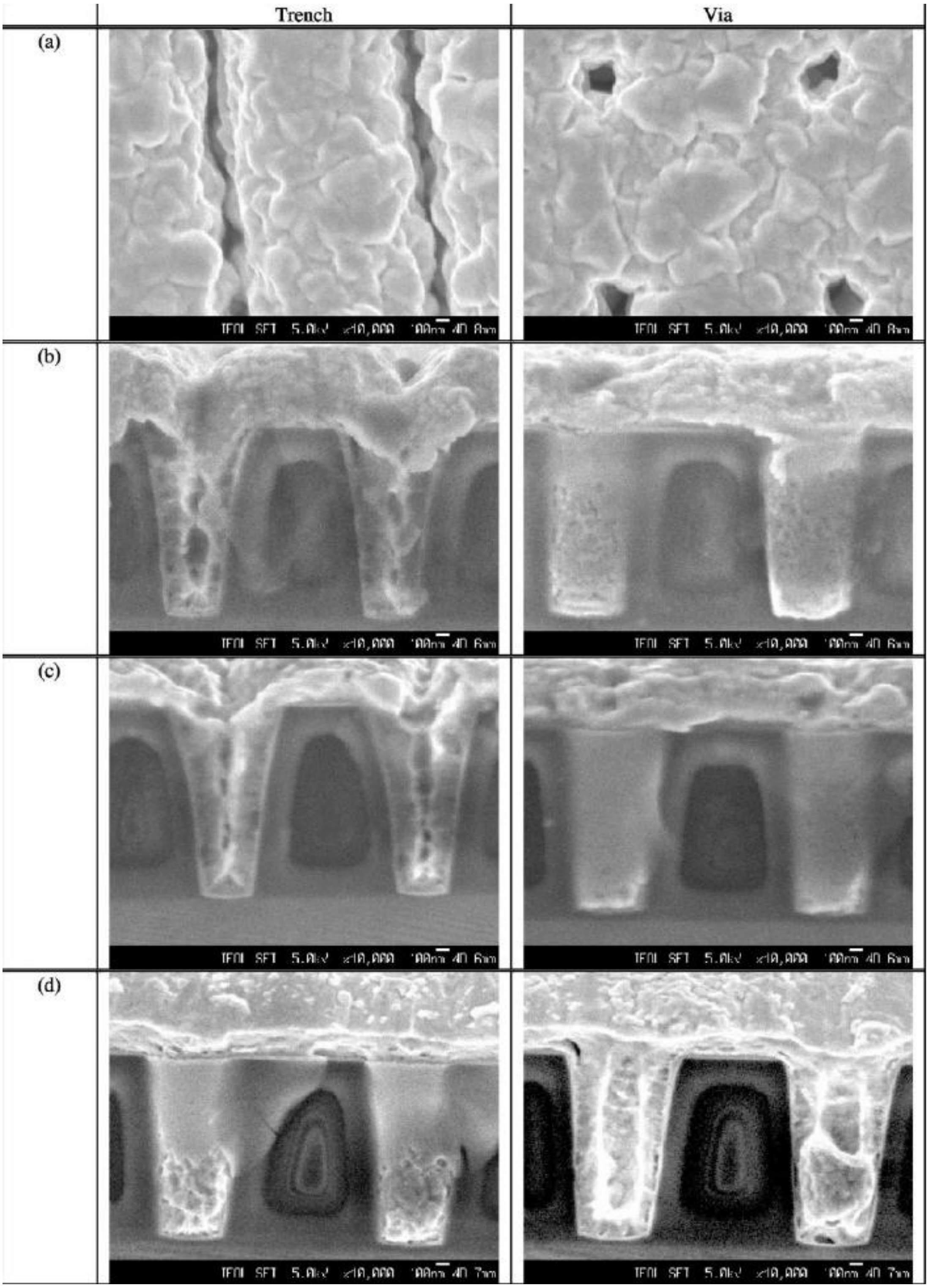

Figure 2.17 : SEM images of line trenches and via holes as a function of different pulse waveform; (a) 3ms on + 0.5 ms off, (b) 6ms on + 2 ms off, (c) 8ms on + 1 ms off, (d) 9.9 ms on + 2.5 ms off [24].

3. EXPERIMENTS AND RESULTS

3.1 Plasma Process

The main focus of plasma process is to create strong boundary layer between polyimide and metal for improving adhesion. Plasma parameters such as plasma gases, duration were optimized and the effects of plasma treatment were investigated with different characterization techniques.

3.1.1 Sample preparation

The surface of the PI films were cleaned with methanol in an ultrasonic water bath for 30 min and then dried in a vacuum oven at room temperature.

3.1.2 Plasma modification

The plasma modification of polyimide substrates, such as Kapton TABE and Kapton HN, was carried out in inductively coupled plasma system, ICP-DRIE Beijing Technol. Science Instruments as shown in Fig. 3.1 before the deposition of Ti/Cu layers. First, the reactor chamber was pumped down to a chamber pressure less than 50 mTorr by mechanical vacuum pump. After rough vacuum was achieved, turbo molecular pump was started to obtain low vacuum. Plasma gases, such as argon or oxygen were fed in to chamber. When the chamber pressure stabilizes, top power and bottom power were applied to create plasma as shown in Fig. 3. 2. After surface treatment of PI films, bottom and top power were turned off. Gases pumped out, the vacuum was broken by opening deflation valve to admit air in to the chamber. Chamber pressure reaches the atmospheric pressure within 2-3 min and plasma treated samples were taken out for characterization. The plasma parameters are given in Table 3.1.

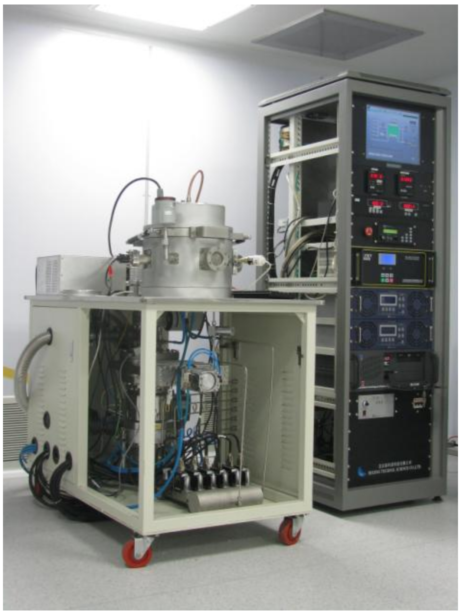

Figure 3.1 : Inductively coupled plasma

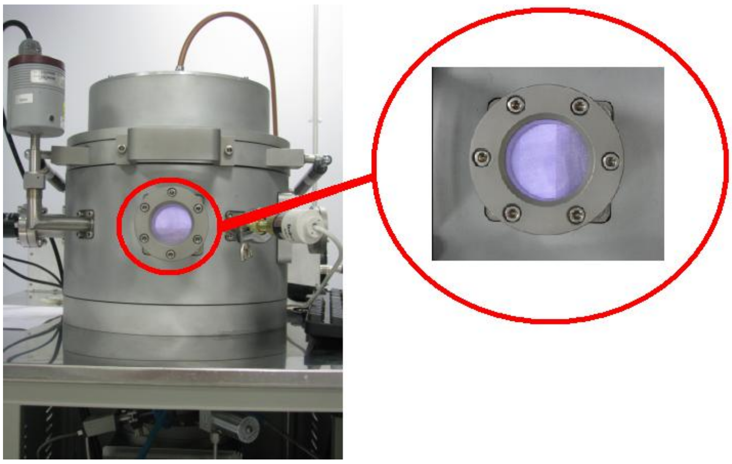

Figure 3.2 : Plasma creation

Table 3.1: The settings for the plasma modification on PI films.

Test	Material	Gas	Flow rate [sccm]	Power [W]	Chamber pressure [mTorr]	Duration [min]
SET 1	Kapton HN	Oxygen	30	40-125	30	0, 1, 3 and 5
SET 2	Kapton TABE	Oxygen	30	40-125	30	0, 1, 3 and 5
SET 3	Kapton TABE	Argon	30	40-125	30	0, 1, 3 and 5
SET 4	Kapton HN	Argon	30	40-125	30	0, 1, 3 and 5

3.1.3 Contact angle measurements

The wettability of the PI films was evaluated by measuring the contact angle between the film surface and a distilled water droplet, using KSV CAM200. An average of ten measurements with a standard deviation below 1 degree were obtained. During the contact angle measurement, we investigated the argon and oxygen plasma effects on different PI films: Kapton TABE and Kapton HN. Fig. 3.3 shows the measured contact angle values of the argon plasma treated Kapton TABE and Kapton HN films at top power of 40W, substrate bias power of 125W and gas flow rate of 30 sccm. While the contact angle of the untreated Kapton TABE was 70.55°, contact angle of the argon plasma treated Kapton TABE films were reduced to 8.37° after 1 min. While the contact angle of the untreated Kapton HN were 68.55°, contact angles of the argon plasma treated Kapton HN films were reduced to 10.16°. after 1 min. After 3 minutes of treatment, the contact angles for both film were reduced to 0°. Fig. 3.4 shows the measured contact angle values of the oxygen plasma treated Kapton TABE and Kapton HN films. The contact angle values of the plasma treated Kapton TABE films were reduced to 0°, after 1 minute of treatment. On the other hand the contact angle values of the plasma treated Kapton HN films were reduced 0° after 3 minutes. According to these contact angle measurement results, it is found that there is not much of a difference between the wettability characteristics of Kapton TABE and Kapton HN films.

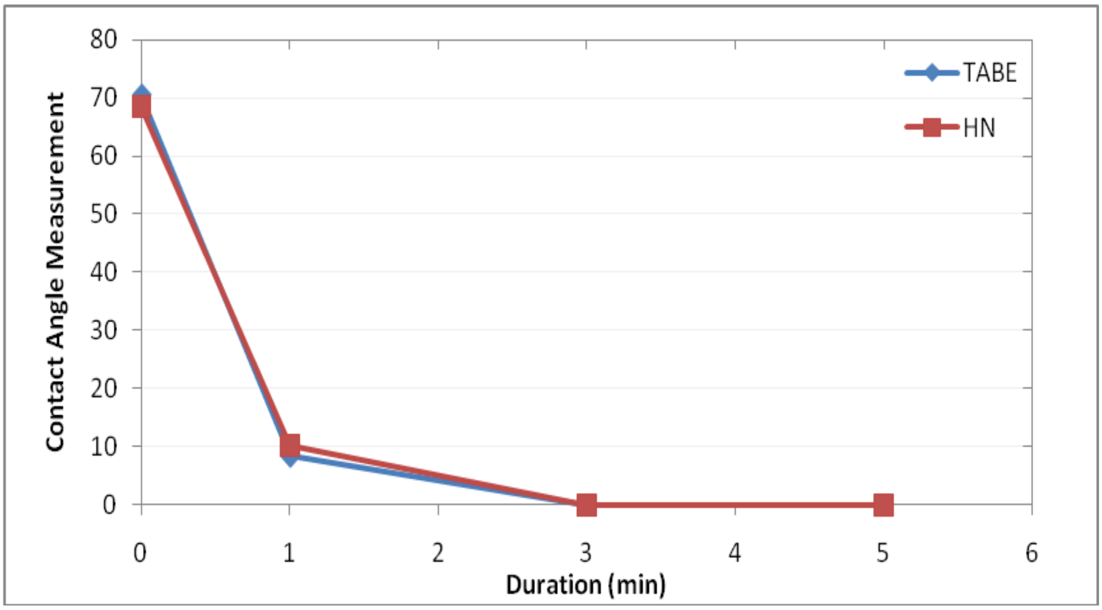

Figure 3.3 : Contact angle values of argon plasma treated Kapton HN and Kapton TABE films as a function of duration.

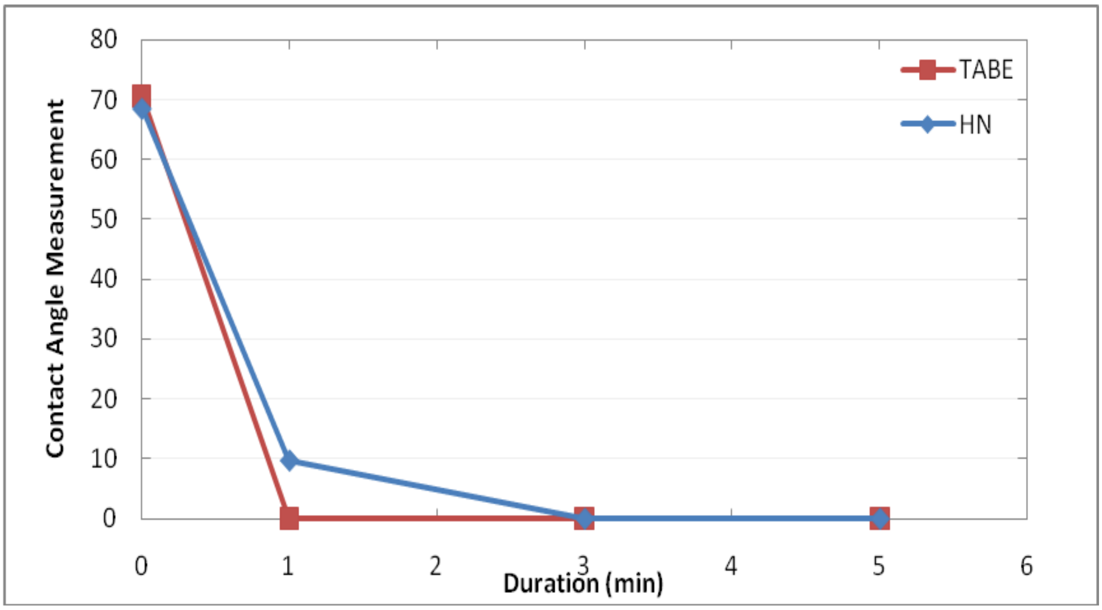

Figure 3.4 : Contact angle values of oxygen plasma treated Kapton HN and Kapton TABE films as a function of duration.

Furthermore, Fig 3.5-3.8 shows the images of the measured contact angle values as a function of duration. The hydrophilic surfaces gives the lower contact angle and shows the higher surface energy. The higher surface energy provides better adhesion strength between metal and polymer**.**

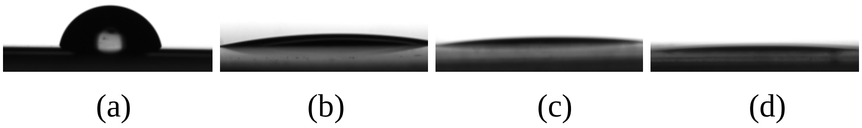
(a) (b) (c) (d)

Figure 3.5 : Contact angle images of argon plasma treated Kapton HN films as a function of a duration (a) unmodified, (b) 1 min, (c) 3 min, (d) 5 min.

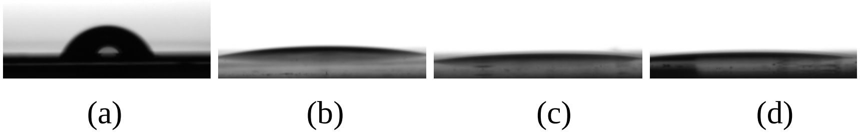
(a) (b) (c) (d)

Figure 3.6 : Contact angle images of argon plasma treated Kapton TABE films as a function of a duration (a) unmodified, (b) 1 min, (c) 3 min, (d) 5 min.

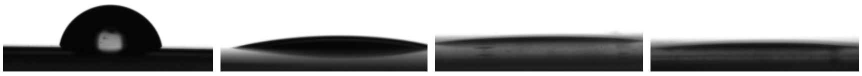

(a) (b) (c) (d)

Figure 3.7 : Contact angle images of oxygen plasma treated Kapton HN films as a function of a duration (a) unmodified, (b) 1 min, (c) 3 min, (d) 5 min.

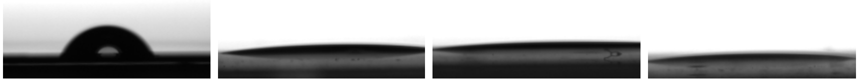

(a) (b) (c) (d)

Figure 3.8 : Contact angle images of oxygen plasma treated Kapton TABE films as a function of a duration (a) unmodified, (b) 1 min, (c) 3 min, (d) 5 min.

3.1.4 AFM analysis

The surface morphologies of the plasma treated PI films were studied by AFM, using Nanomagnetics Instruments. For each sample, an area of 4x4 μm was scanned using tapping mode. The AFM observations was carried out at ambient pressure and room temperature. The mean square root of roughness was calculated. Fig. 3.9 shows 4.0 x 4.0 μm^2 AFM image of the argon treated PI films as a function of duration. Accelerated oxygen and argon ions roughen the surface of the Kapton TABE polyimide films. Root-mean-squared (RMS) roughness values of the untreated Kapton TABE film was 1.58 nm. The AFM image of the 1 min. argon treated polyimide films cannot be seen in Fig. 3.9, because the cantilever sticked the 1 min. argon treated samples. To determine the 1 minute argon treated sample roughness, the roughness of the sample was measured on different regions of the sample and the average surface roughness was calculated. The RMS roughness values of the argon treated Kapton TABE films at the duration of 1, 3, 5 min were increased to 7.3, 23.39, and 32.21 nm, respectively. As seen in Fig.3.9, increased duration roughens the surface by increased argon bombardments. Grass like surface morphologies with increased surface roughness were observed as duration increases. Fig. 3.10 shows 4.0 x 4.0 μm^2 AFM image of the oxygen treated PI films as a function of duration. The RMS roughness values of the oxygen treated Kapton TABE films at the duration of 1, 3, 5 min were increased to 7.05, 18.96, and 28.55 nm, respectively. Increased duration roughens the surface by increased oxygen bombardments. Much more cross linked surface morphologies with increased surface roughness were observed as the duration increases. Fig. 3.11 and Fig. 3.12 shows the measured contact angle values of the argon and oxygen plasma treated Kapton TABE films together with the RMS roughness values obtained from the AFM images in Fig. 3.9 and Fig. 3.10. The results show that the large increase in the RMS roughness causes to decrease in contact angles. Nano scale roughness increases the total surface area and as a result reduced contact angles.

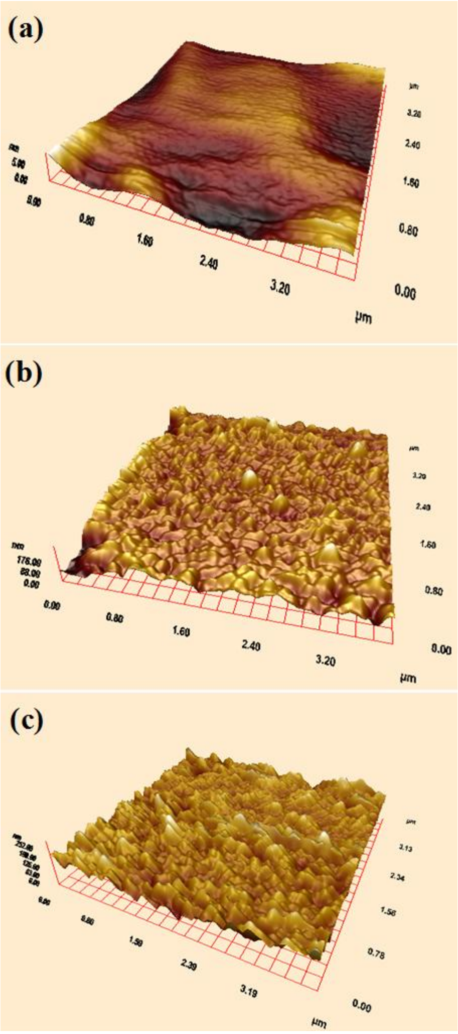
(a)
0.80
1.60
2.40
3.20
µm
3.20
2.40
1.60
0.80
0.00
(b)
176.00
88.00
0.00
0.00
0.80
1.60
2.40
3.20
µm
3.20
2.40
1.60
0.80
0.00
(c)
0.80
1.59
2.39
3.19
µm
3.13
2.34
1.56
0.78
0.00

Figure 3.9 : 4.0 x 4.0 µm^2 AFM image of argon plasma treated Kapton TABE surfaces as a function of duration; (a) untreated, (b) 3 min, (c) 5 min.

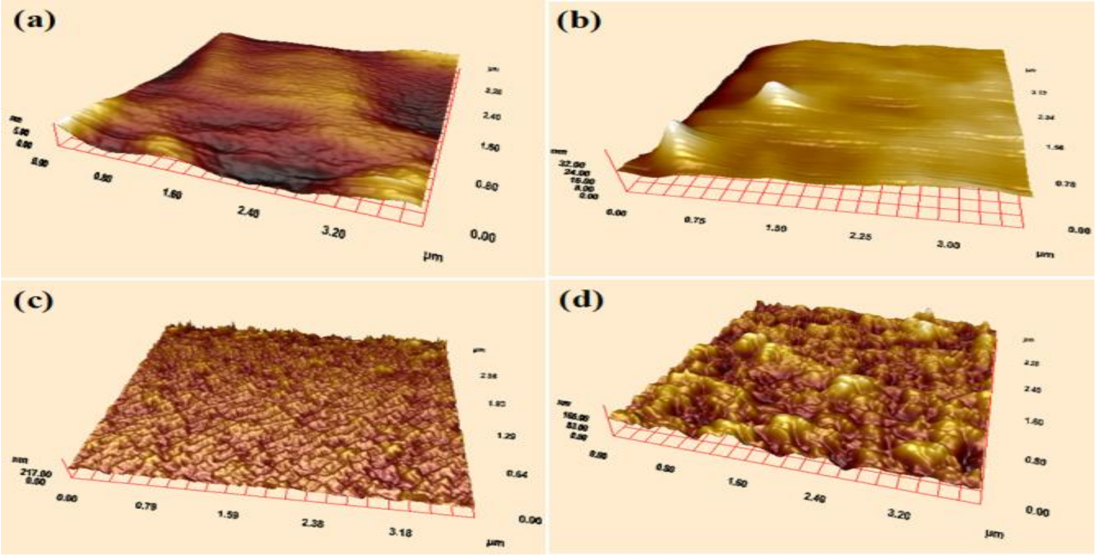
(a)
0.00
0.80
1.60
2.40
3.20
µm
(b)
0.00
0.75
1.50
2.25
3.00
µm
(c)
0.00
0.79
1.59
2.38
3.18
µm
(d)
0.00
0.80
1.60
2.40
3.20
µm

Figure 3.10 : 4.0 x 4.0 µm^2 AFM image of oxygen plasma treated Kapton TABE surfaces as a function of duration; (a) untreated, (b) 1 min, (c) 3 min, (d) 5 min.

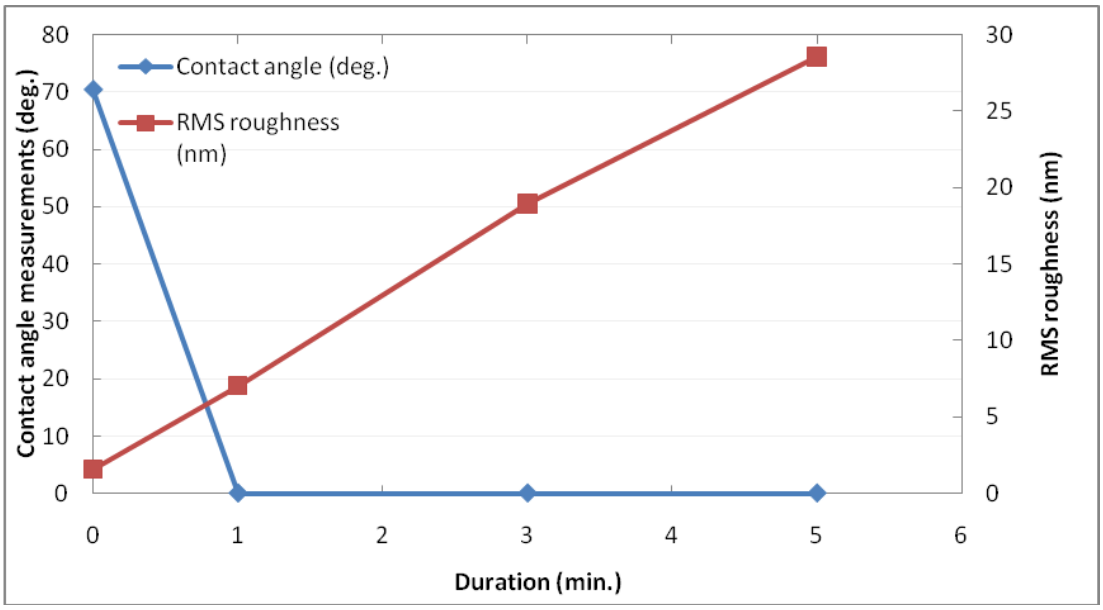

Figure 3.11 : Relationship between contact angle and RMS roughness of oxygen plasma treated Kapton TABE films as a function of duration.

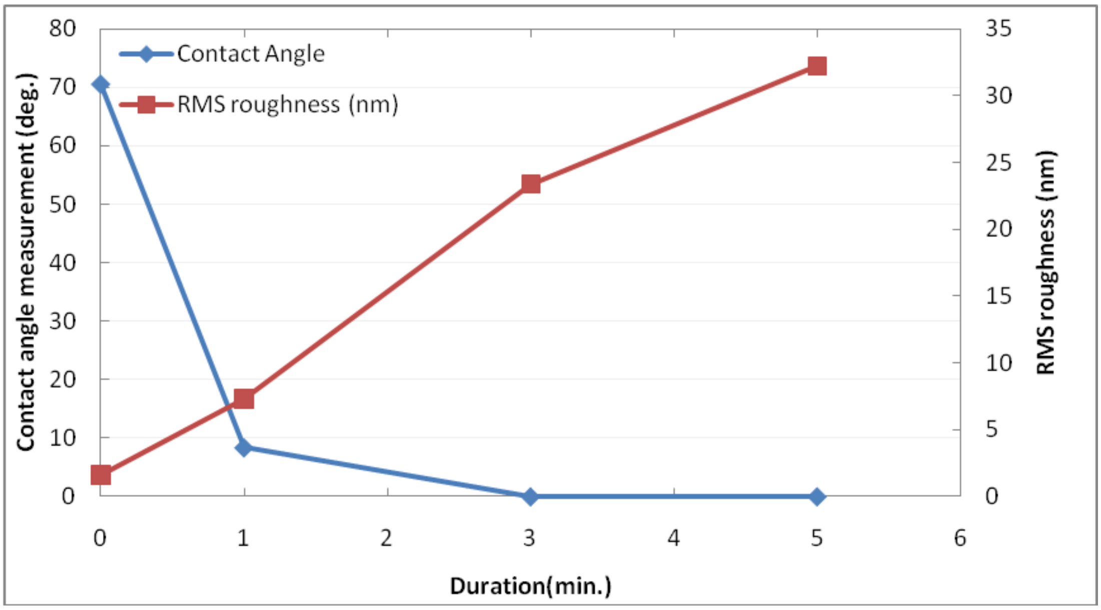

Figure 3.12 : Relationship between contact angle and RMS roughness of argon plasma treated Kapton TABE films as a function of duration.

3.1.5 FTIR analysis

FTIR spectra of plasma treated PI films were obtained using Perkin Elmer spectrometer. The scans were shown from 650 to 4000 cm^{-1} and required 40s to complete. Fig. 3.13 indicates the chemical composition of argon plasma treated Kapton TABE films as a function of duration. As seen in Fig. 3.13, the bands observed around 717, 1083, 1238, 1350, 1500, 1707, 1774, were assigned respectively to the C=O bending, C-O-C stretching, C-O-C asymmetrical stretching, C-N stretching, aromatic C=C ring stretch., C=O symmetrical stretching and C=O asymmetrical stretching. The chemical bands of polyimide conform with the FTIR analysis polyimide done by other researchers [11,28-30]. The C=O bending and symmetrical stretching peaks at 717 and 1770 cm^{-1} and C-O-C stretching and asymmetrical stretching peaks at 1083 and 1238 cm^{-1} become stronger at one minute treatment and become weaker with increasing time. C-N chemical bond gives strong peaks (corresponding to 1350 cm-^{1}) at one minute duration and decreases with increasing time. Also, new peak arose at 3485 cm^{-1} (corresponding to O-H stretching) after one minute argon treatment. Moreover, new peak at 3746 cm^{-1} (corresponding to N-H stretching) is observed on the argon treated polyimide for one minute.

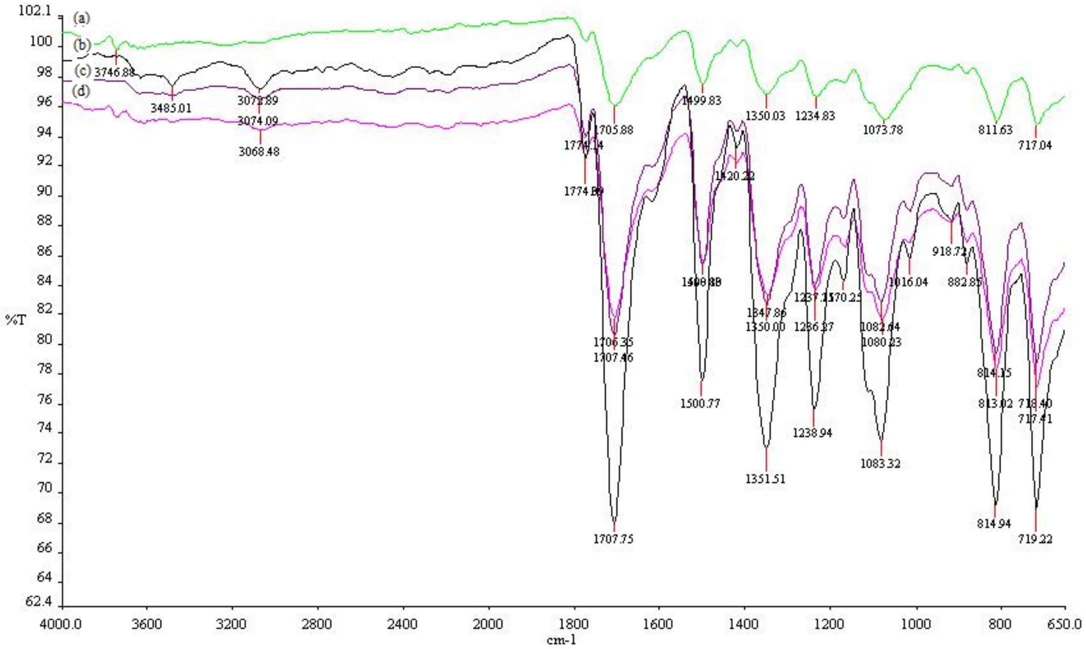

Figure 3.13 : FTIR spectra of argon plasma treated Kapton TABE films as a function of duration (a) 5 min (b) 1 min (c) 0 min (d) 3 min

These changes indicate that chemical structure of polyimide films change after plasma treatment. The formation of O-H functional groups show that reactive free radical colloid with the surface of PI films [12]. Previous studies reported that the increased number of functional groups such as C=O, C-O-C by the plasma treatment improve the adhesion strength between metal and polymer [10,7,5,6]. In the light of previous studies, we can say that argon treatment for one minute duration creates more functional groups on surface. This oxygen containing functional groups interact with the metals to form chelate-like complexes and provides good adhesion between metal and polyimide. FTIR spectra of the oxygen treated polyimide films could not obtained. The analysis of the FTIR method is inadequate for the oxygen plasma modification.

3.2 Magnetron Sputtering

The main focus of sputtering process is to create an adhesion layer and seed layer prior to electroplating. Deposition of Ti and Cu layers on polyimide substrate was carried out in physical vapour deposition system, Beijing Technol. Science Instruments as shown in Fig. 3.14.

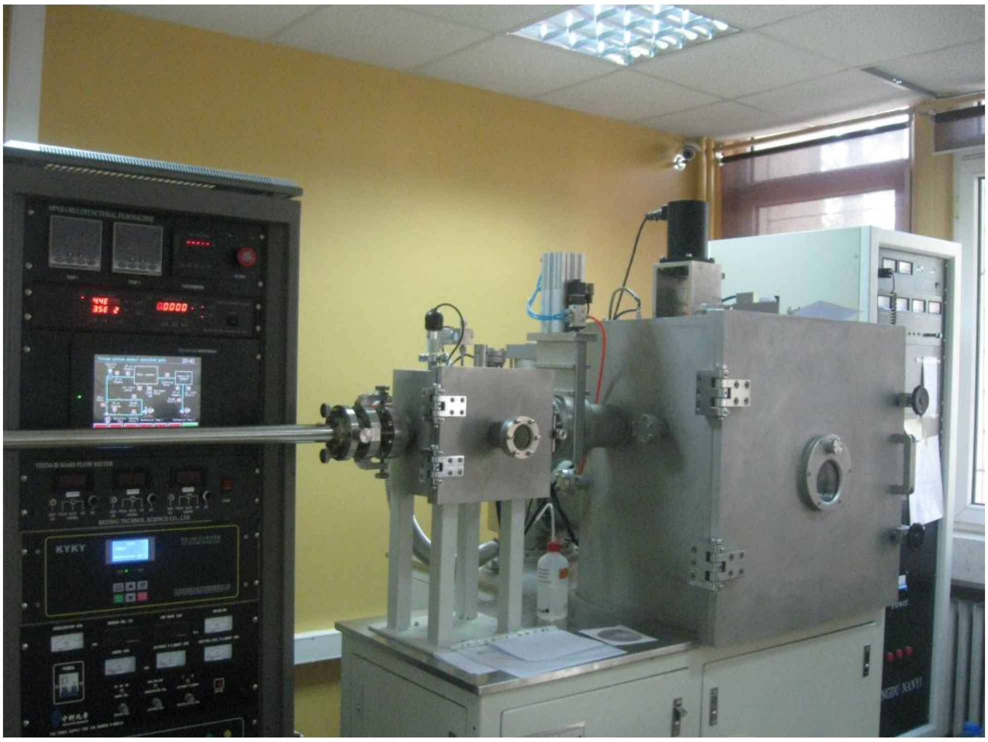

Figure 3.14 : Physical vapor deposition system

This functional PVD system has different deposition systems like e-beam, thermal evaporation and DC magnetron sputtering. Prior deposition, the reactor chamber was pumped down to a chamber pressure less than 3 Pa by mechanical vacuum pump. After rough vacuum was achieved, turbo molecular pump was started to obtain low vacuum less than 10^{-3} Pa and then argon gas fed in to the chamber. When the chamber pressure reached the set point, the power value was adjusted. Then shutter was opened and a visible glow discharge was observed. Positive ions in the plasma strike and eject the negative target atoms with momentum transfer.

Target atoms pass the discharge region and deposit on the substrate. After deposition of metal on the substrate, shutter was closed. Gases pumped out, the vacuum was broken by opening deflation valve to admit air in to the chamber. Chamber pressure reaches the atmospheric pressure within 15-20 min.

3.2.1 Deposition of Ti and Cu seed layer on the polyimide substrate

In this study, Ti was selected as an adhesion promoting layer between the polyimide and copper. To determine sufficient power for ejecting the Ti atoms on the cathode surface, five different power values were compared. The deposition parameters are given in Table 3.2.

Table 3.2: The settings for Ti deposition on PI films.

Test	Flow rate [sccm]	Power [W]	Chamber pressure [Pa]	Duration [min]
SET 1	65	100 W	0.9	15 min
SET 2	65	150 W	0.9	15 min
SET 3	65	200W	0.9	15 min
SET 4	65	250 W	0.9	15 min
SET 5	65	300 W	0.9	15 min

After experiments, it was seen that power of 100W, 150W, 200W are inadequate for ejecting titanium atoms on the cathode surface. On the other hand, the power of 150W is sufficient to eject the copper atoms on the cathode surface during sputtering process. Because the sputtering yield of the titanium is very low, when we compare with the sputter yield of copper.

For determining the thickness of the Ti and Cu layers, the small pieces of Si wafers were metalized with polyimide samples. Because polyimide is a flexible material and it causes problem when measuring thickness by profilometre. After thickness measurements of the Si by profilometre, it was seen that the deposition rates of titanium was 12 nm/min at power of 250 W, flow rate of 65 sccm, chamber pressure of 0.9 Pa and the deposition rate of copper 40 nm/min at power of 150W, flow rate of 65 sccm, chamber pressure of 0.9 Pa. The deposition parameters are given in Table 3.3.

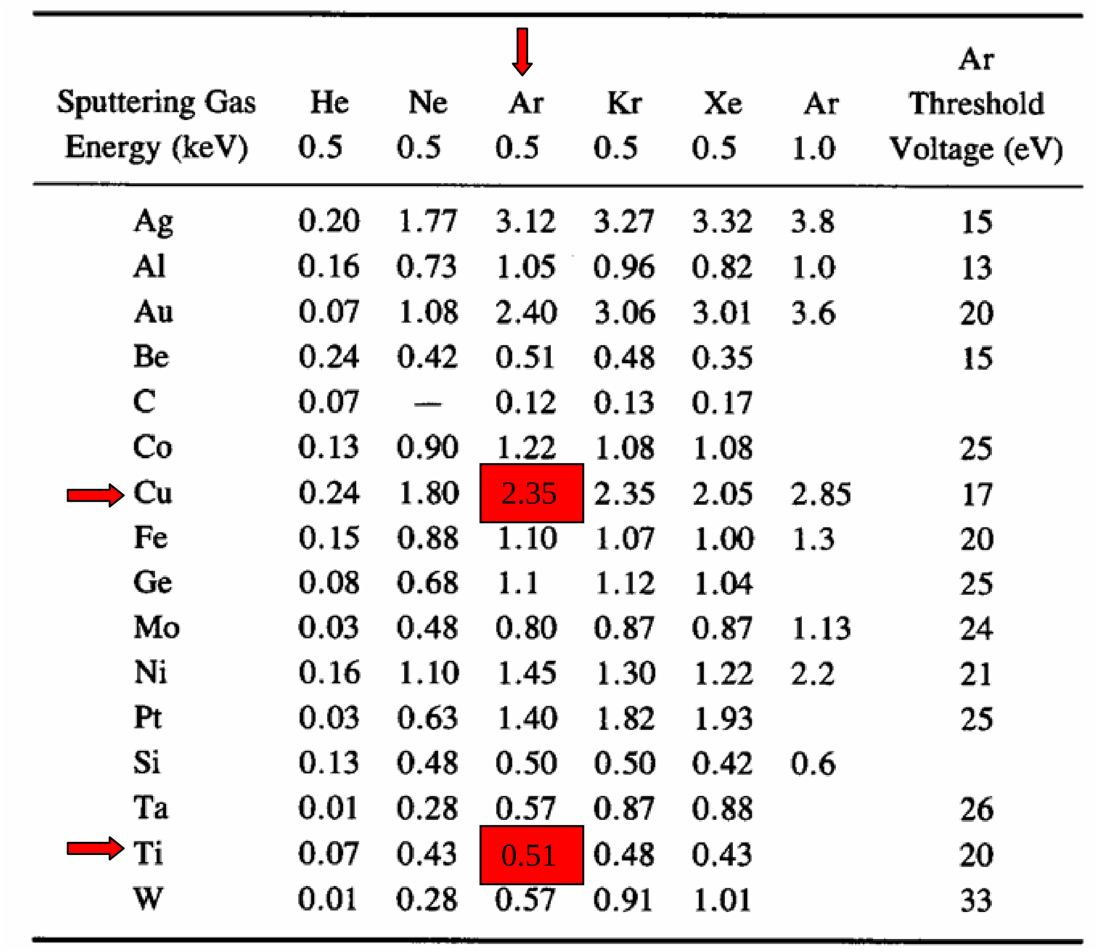

Sputtering Gas Energy (keV)	He 0.5	Ne 0.5	Ar 0.5	Kr 0.5	Xe 0.5	Ar 1.0	Ar Threshold Voltage (eV)
Ag	0.20	1.77	3.12	3.27	3.32	3.8	15
Al	0.16	0.73	1.05	0.96	0.82	1.0	13
Au	0.07	1.08	2.40	3.06	3.01	3.6	20
Be	0.24	0.42	0.51	0.48	0.35		15
C	0.07	—	0.12	0.13	0.17		
Co	0.13	0.90	1.22	1.08	1.08		25
Cu	0.24	1.80	2.35	2.35	2.05	2.85	17
Fe	0.15	0.88	1.10	1.07	1.00	1.3	20
Ge	0.08	0.68	1.1	1.12	1.04		25
Mo	0.03	0.48	0.80	0.87	0.87	1.13	24
Ni	0.16	1.10	1.45	1.30	1.22	2.2	21
Pt	0.03	0.63	1.40	1.82	1.93		25
Si	0.13	0.48	0.50	0.50	0.42	0.6	
Ta	0.01	0.28	0.57	0.87	0.88		26
Ti	0.07	0.43	0.51	0.48	0.43		20
W	0.01	0.28	0.57	0.91	1.01		33

Figure 3.15 : Sputtering yields data for metals [31].

Table 3.3: The settings for Cu deposition on PI films.

Metal	Flow rate [sccm]	Power [W]	Chamber pressure [Pa]	Duration [min]	Thickness [µm]
Ti	65	250 W	0.9	10 min	120 nm
Cu	65	150 W	0.9	5 min	200 nm

3.3 Magnetron Sputtering

Pulse plating parameters such as current density and pulse waveforms were optimized and the effects of current density and pulse waveforms on films were investigated with scanning electron microscopy.

As seen in Fig. 3.16, electroplating setup consists of:

- an anode; 5x5 cm^2 %99.99 pure copper sheet

- an electrolyte solution which includes; 0.3 M CuSO4, 2M H2SO4, 1.4x 10^{-3} HCl
- Microstar Dynatronix pulse plating instrument,
- a cathode; 3 cm^2 Cu/Ti/polyimide film
- cell
- aquarium pump
- flow meter; flow rate adjusted to the 4 l/h

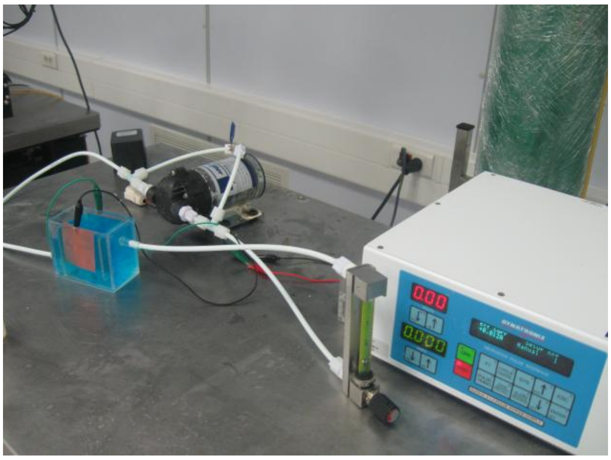

Figure 3.16 : The experimental setup.

During electroplating, the concentration of the ions near the cathode decreases, so recirculation system was used to determine the homogenous electrolyte. Electrolyte was circulated by aquarium pump and the flow rate of the electrolyte was determined by flow meter. All electroplating experiments were carried out at the room temperature and pH 3. Other electroplating parameters are given in Table 3.4.

Table 3.4: The settings for the copper electroplating on Cu/Ti/PI films.

Test	**$I_{forward}$**	**$I_{reverse}$**	**$I_{average}$**	**on time**	**off time**	**duty cycle**
SET 1	15 mA	15 mA	12 mA	90 ms	10 ms	100 ms
	30 mA	30 mA	24 mA	90 ms	10 ms	100 ms
	45 mA	45 mA	36 mA	90 ms	10 ms	100 ms
	60 mA	60 mA	48 mA	90 ms	10 ms	100 ms
SET 2	30 mA	30 mA	24 mA	90 ms	10 ms	100 ms
	30 mA	30 mA	18 mA	80 ms	20 ms	100 ms
	30 mA	30 mA	12 mA	70 ms	30 ms	100 ms
	30 mA	30 mA	6 mA	60 ms	40 ms	100 ms

3.3.1 Effect of current density

The first sets of experiments were designed for investigating the effect of current density on film properties. The surface characteristics of the electroplated copper films were characterized by SEM and profilometer. As seen in Fig. 3.17-3.20, SEM micrographs of the electroplated copper show that the smooth surface was obtained with a mean current density of 8 mA/cm^2. Analysis of the roughness by profilometer confirms this observation. The surface roughness was obtained using Veeco Dektak 6M stylus profiler.

Table 3.5: The average roughness of the copper films as a function of the current density.

Test	$I_{forward}$	$I_{reverse}$	$I_{average}$	on time	off time	duty cycle	Ra
SET 1	15 mA	15 mA	12 mA	90 ms	10 ms	100 ms	0.500
	30 mA	30 mA	24 mA	90 ms	10 ms	100 ms	0.031
	45 mA	45 mA	36 mA	90 ms	10 ms	100 ms	0.054
	60 mA	60 mA	48 mA	90 ms	10 ms	100 ms	0.074

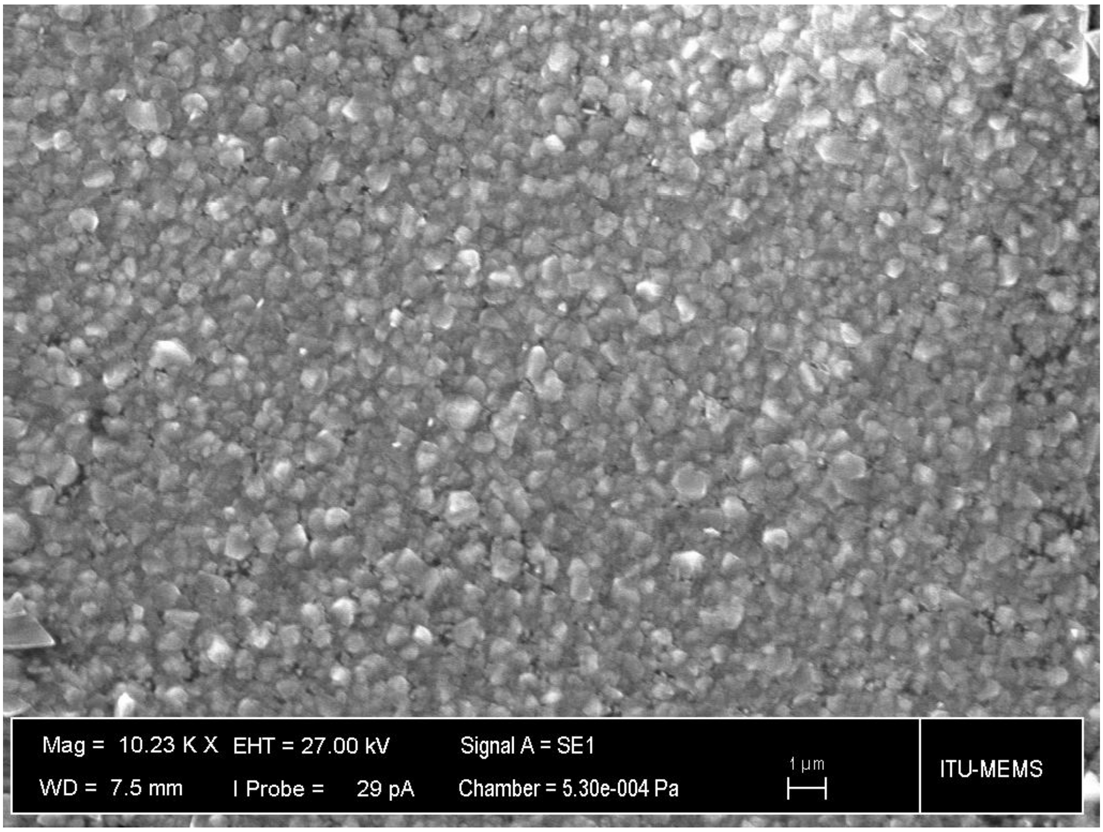

Figure 3.17 : SEM micrographs of electroplated copper at a mean current density of 4mA/cm^2

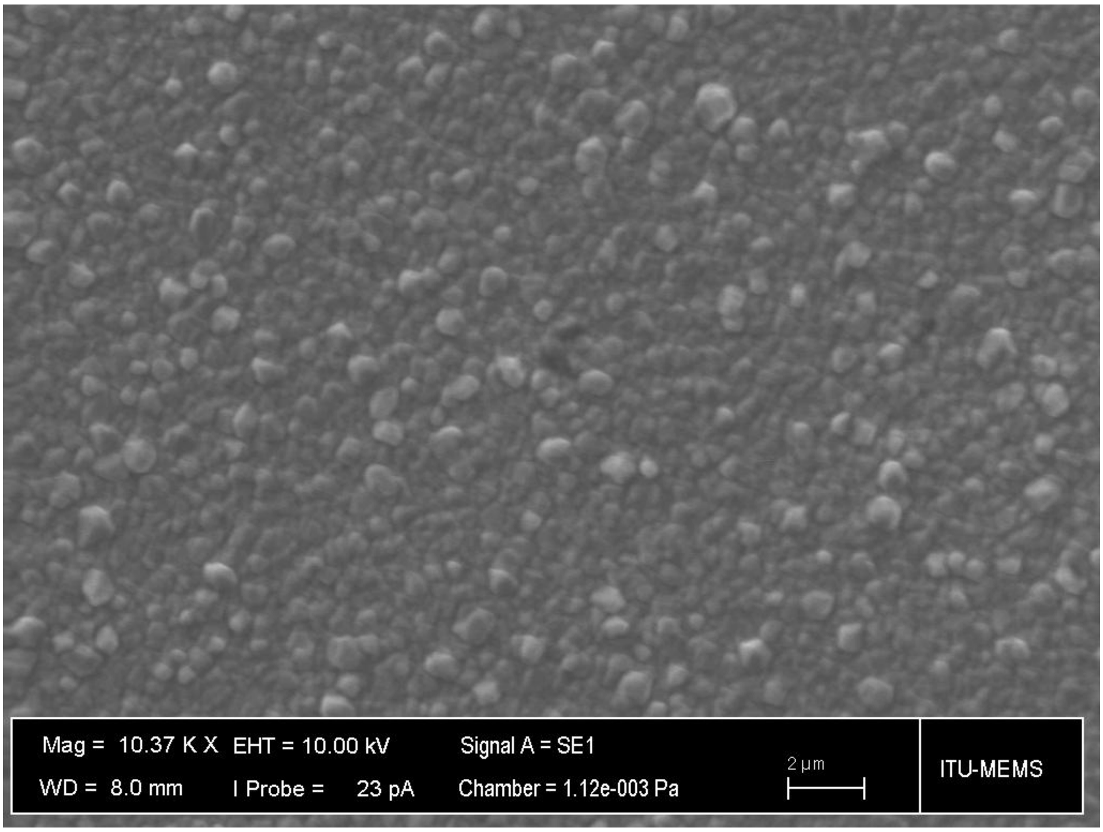
Mag = 10.37 K X
EHT = 10.00 kV
Signal A = SE1
2 µm
ITU-MEMS
WD = 8.0 mm
I Probe = 23 pA
Chamber = 1.12e-003 Pa

Figure 3.18 : SEM micrographs of electroplated copper at a mean current density of 8 mA/cm^2

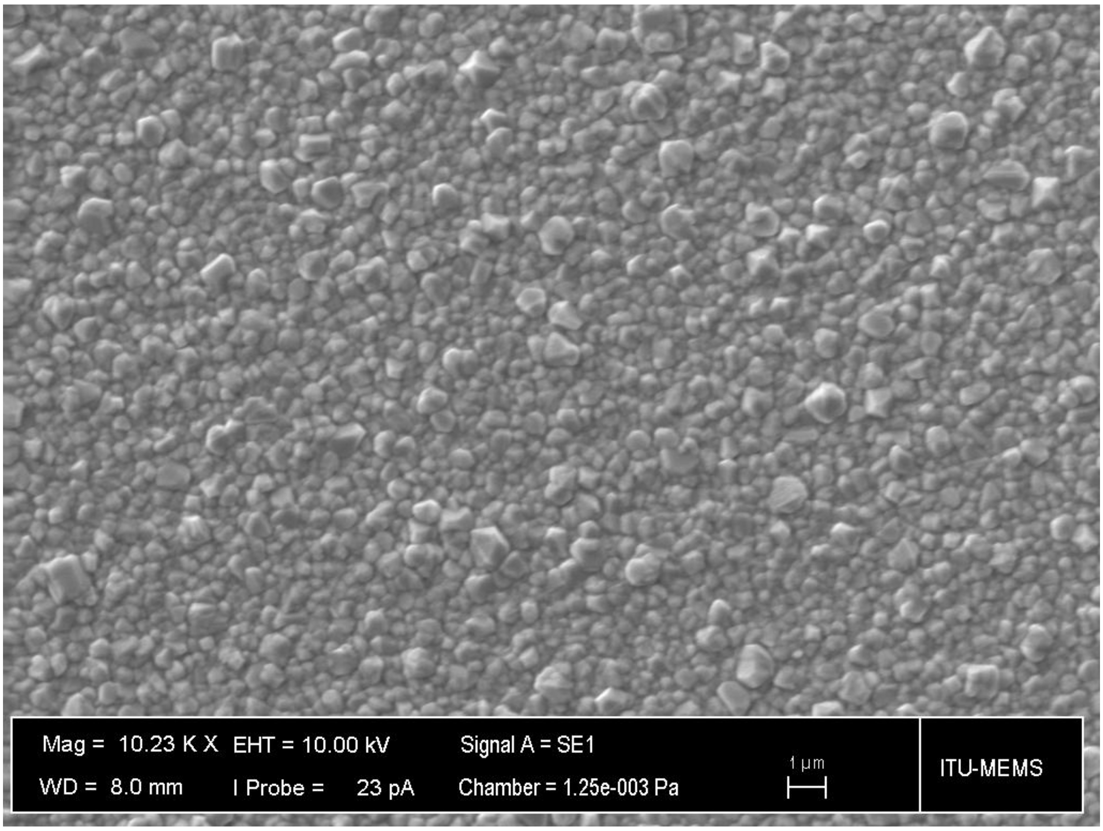
Mag = 10.23 K X
EHT = 10.00 kV
Signal A = SE1
1 µm
ITU-MEMS
WD = 8.0 mm
I Probe = 23 pA
Chamber = 1.25e-003 Pa

Figure 3.19 : SEM micrographs of electroplated copper at mean current density of 12 mA/cm^2

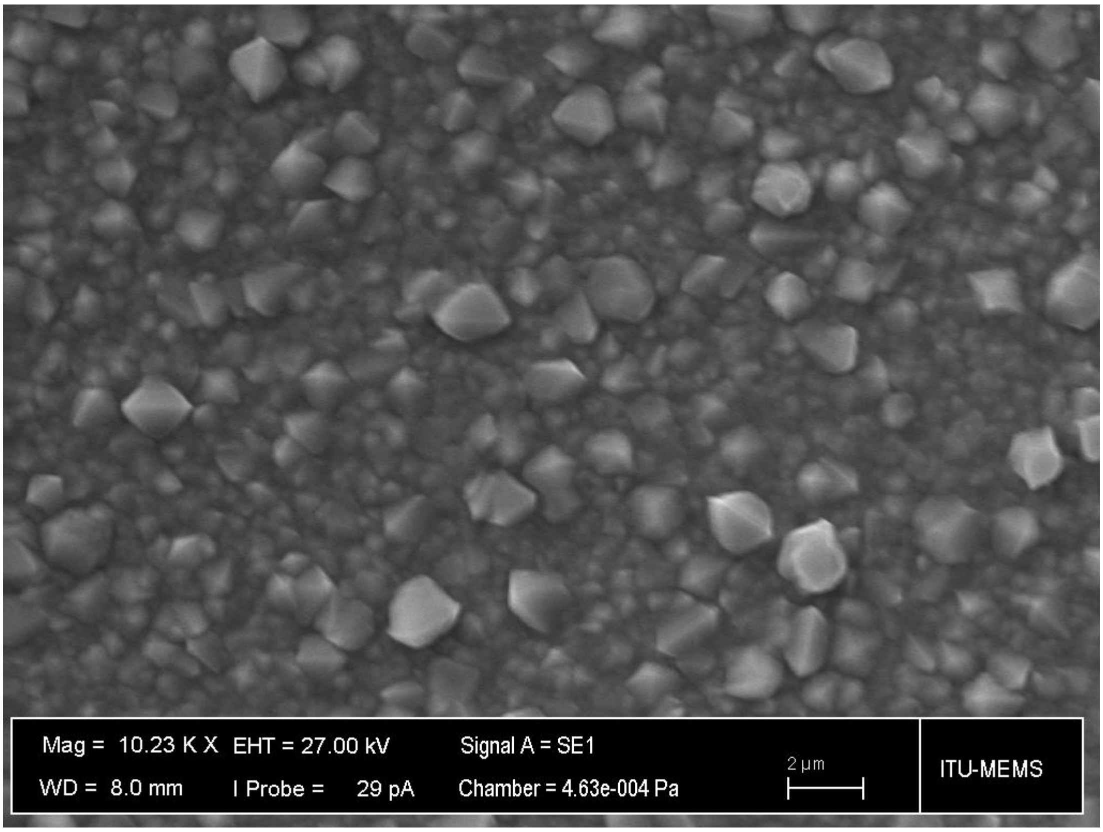
Mag = 10.23 K X
EHT = 27.00 kV
Signal A = SE1
WD = 8.0 mm
I Probe = 29 pA
Chamber = 4.63e-004 Pa
2 µm
ITU-MEMS

Figure 3.20 : SEM micrographs of the electroplated copper at a mean current density of 16 mA/cm^2

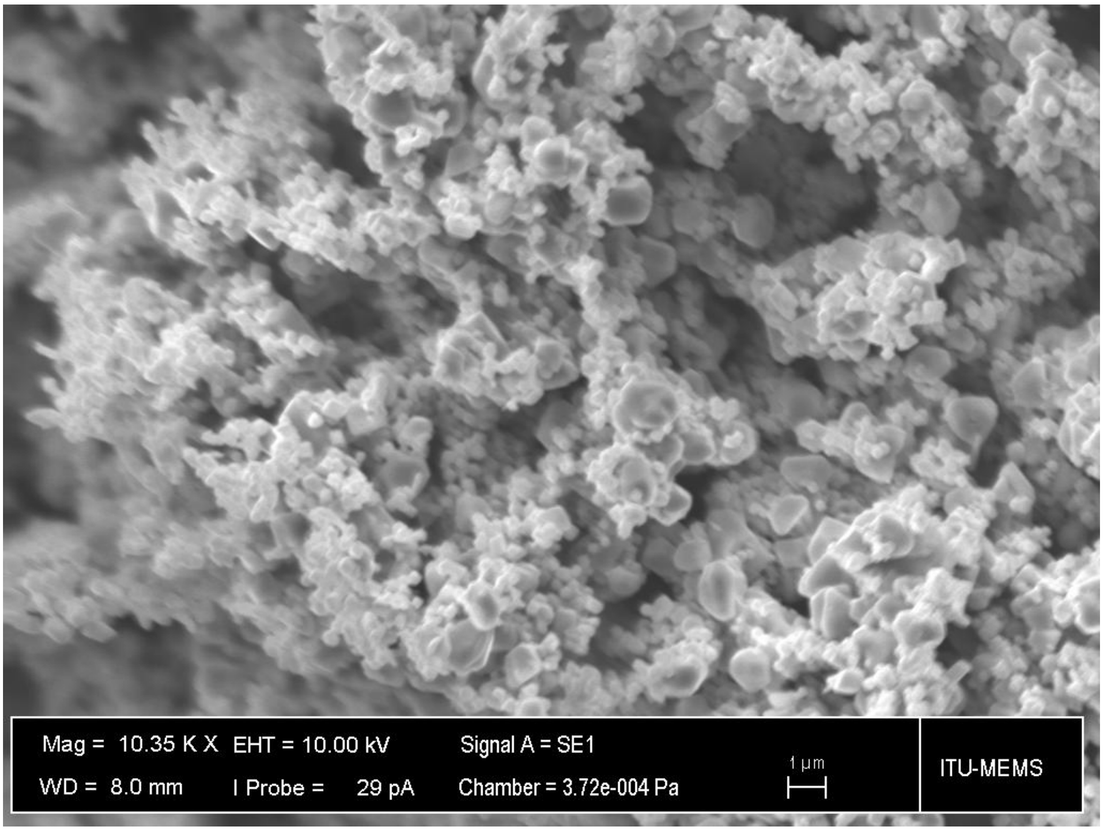
Mag = 10.35 K X
EHT = 10.00 kV
Signal A = SE1
WD = 8.0 mm
I Probe = 29 pA
Chamber = 3.72e-004 Pa
1 µm
ITU-MEMS

Figure 3.21 : SEM micrographs of the electrplated copper at a mean current density of 20 mA/cm^2

When the current density exceeded the 16 mA/cm^2, the formation of hydrogen bubbles were observed on the cathode surface. This causes porous surface and increases the darkness of the film.

3.3.2 Effect of pulse waveforms

The second sets of experiments were designed for investigating the effect of pulse waveforms on film properties. The surface characteristics of the electroplated copper films were characterized by SEM. The current was alternatively turned on and off in during pulse cycle. During on period in every pulse cycle, new nucleation occurs at high energy sites, thus new grains grow continually and the negatively charged layer is formed around the cathode during electroplating process. During off period in every pulse cycle, this layer discharge and provides uniform bath composition. By this way, ions easily reach the cathode surface. As seen in Fig. 3.22 to 3.25, the high average current density causes the greater grain growth of copper grains. The greatest growth of copper grains can be seen in Fig. 3.25. On and off period should be balanced, on the other hand, the secondary growth of copper grains can be observed as seen in Fig. 3.22 to 3.24. Also these secondary growth of copper grains increases with the increased mean current density. The smooth surface was obtained at pulse waveform of 90 ms on and 10 ms off with a current density of 8 mA/cm^2 because on and off periods were balanced.

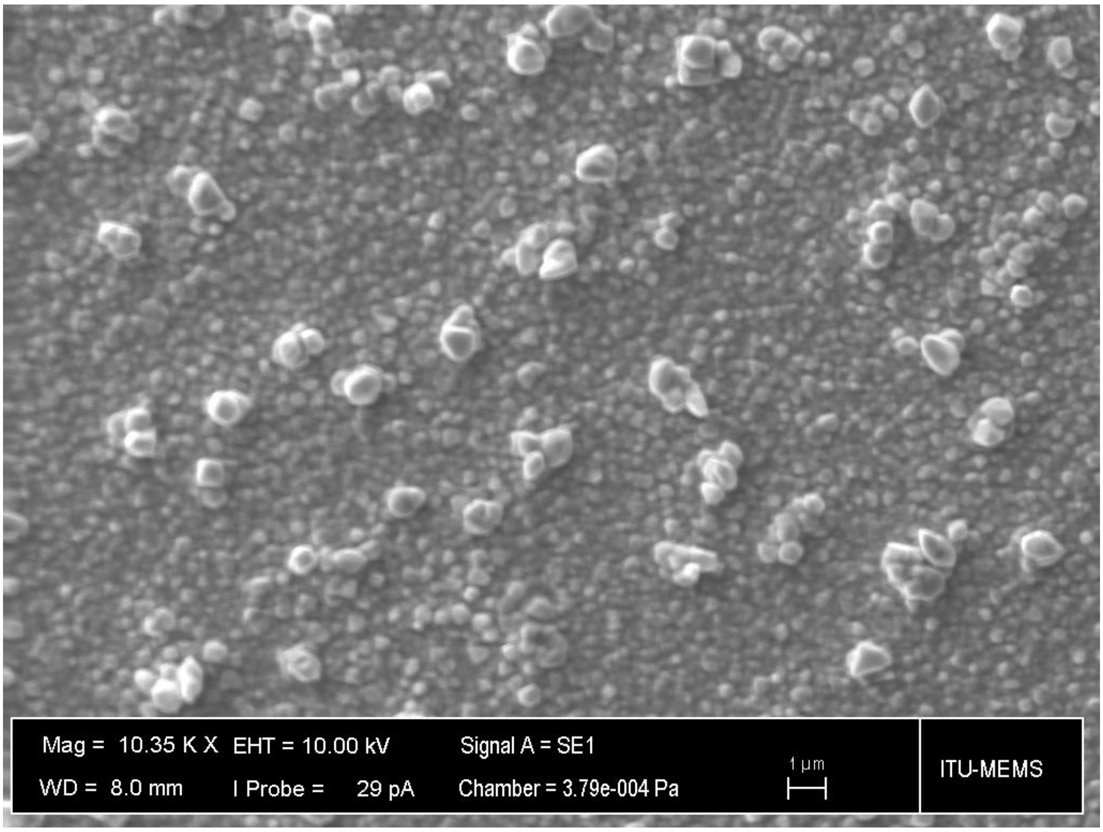
Mag = 10.35 K X
EHT = 10.00 kV
Signal A = SE1
WD = 8.0 mm
I Probe = 29 pA
Chamber = 3.79e-004 Pa
1 µm
ITU-MEMS

Figure 3.22 : SEM micrograph of the electroplated copper at pulse waveform of 60 ms on + 40 ms off and a current density of 2 mA/cm^2

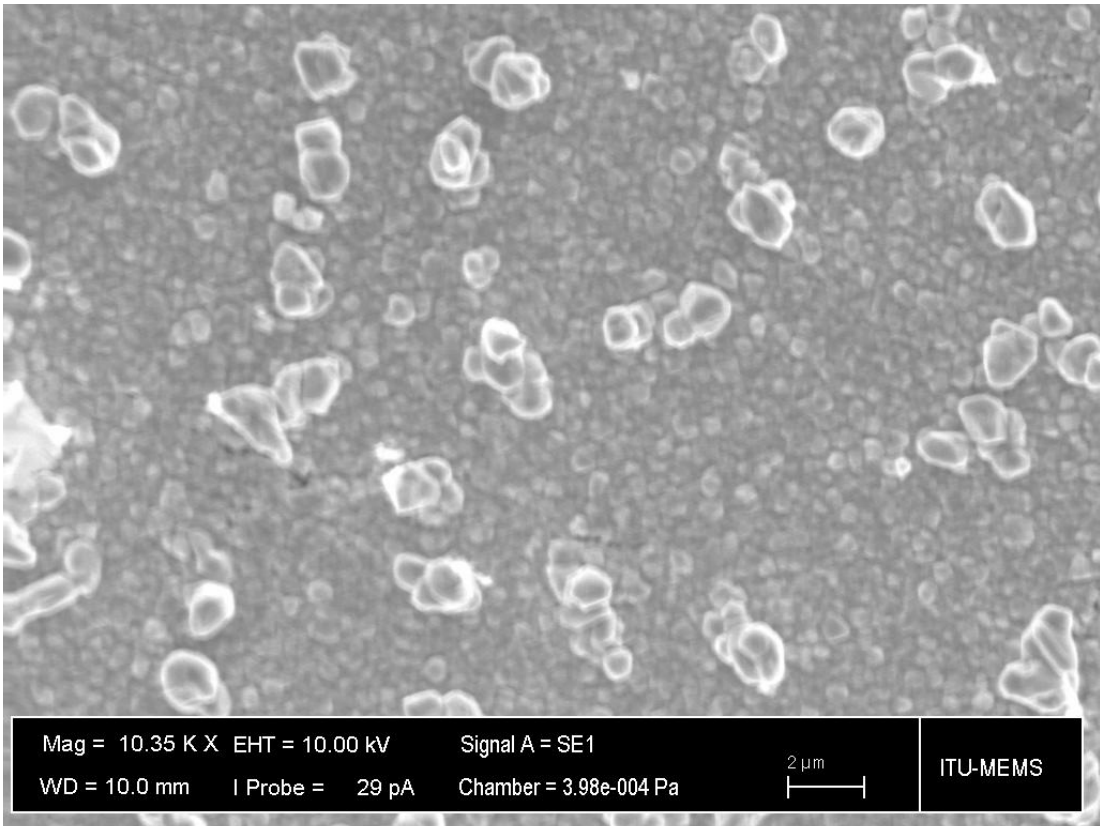
Mag = 10.35 K X
EHT = 10.00 kV
Signal A = SE1
WD = 10.0 mm
I Probe = 29 pA
Chamber = 3.98e-004 Pa
2 µm
ITU-MEMS

Figure 3.23 : SEM micrograph of the electroplated copper at pulse waveform of 70 ms on + 30 ms off and a cuurent density of 4 mA/cm^2

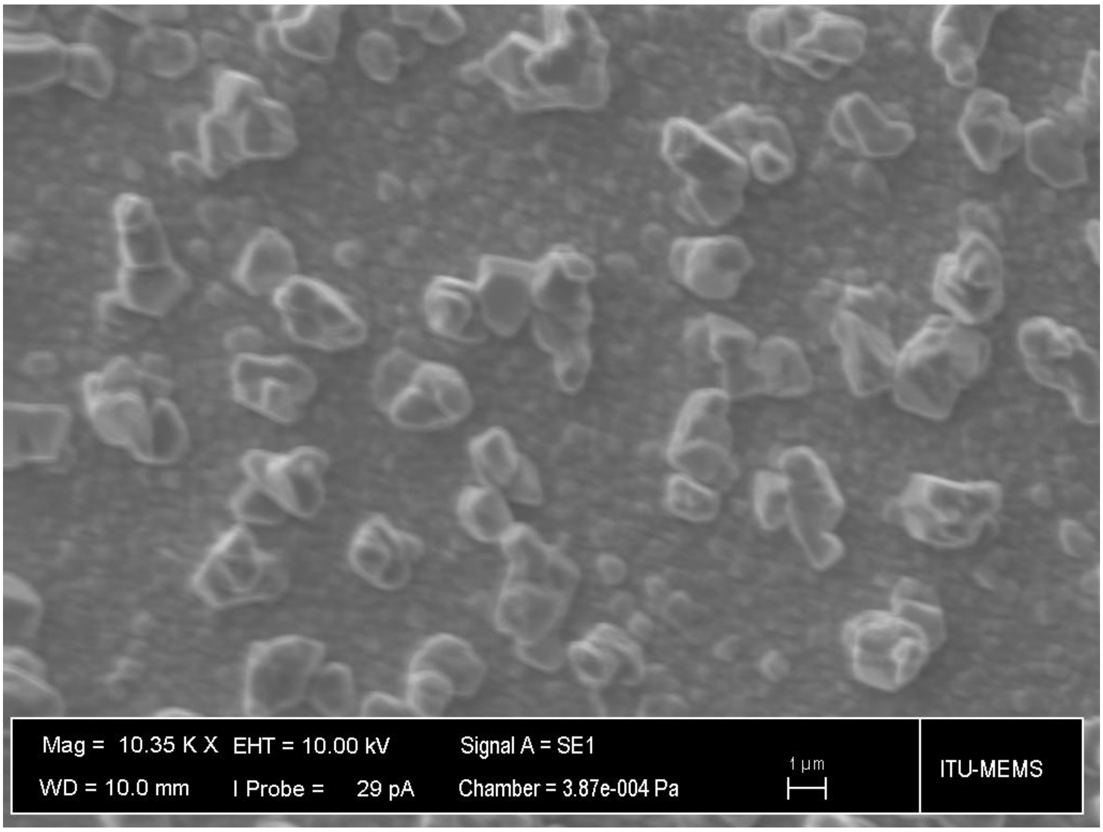
Mag = 10.35 K X
EHT = 10.00 kV
Signal A = SE1
WD = 10.0 mm
I Probe = 29 pA
Chamber = 3.87e-004 Pa
1 μm
ITU-MEMS

Figure 3.24 : SEM micrograph of the electroplated copper at 80 ms on + 20 ms off and a current density of 6 mA/cm^2

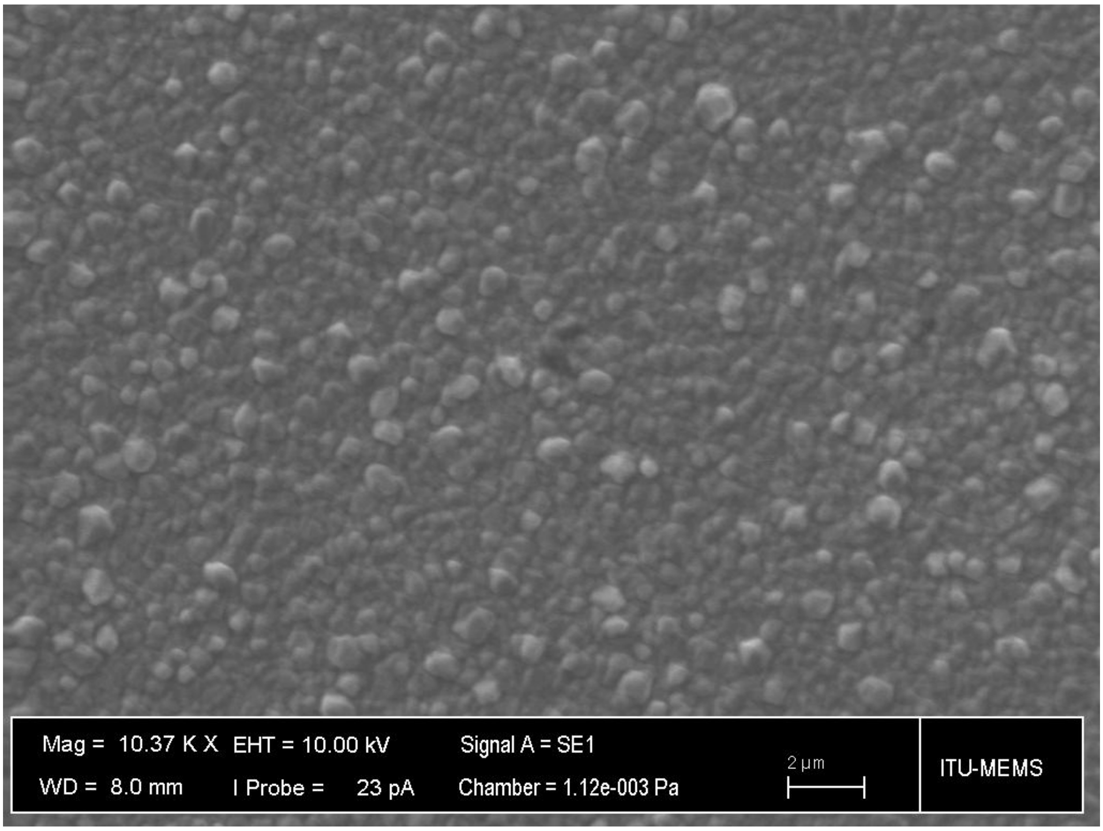
Mag = 10.37 K X
EHT = 10.00 kV
Signal A = SE1
WD = 8.0 mm
I Probe = 23 pA
Chamber = 1.12e-003 Pa
2 μm
ITU-MEMS

Figure 3.25 : SEM micrograph of the electroplated copper at 90 ms on + 10 ms off and a current density of 8 mA/cm^2

4. CONCLUSION AND RECOMMENDATIONS

In this work, the results demonstrated that the argon and oxygen plasma modification are the good modification methods. Because the adhesion performance of the sputtered layer on polyimide films is strongly affected by the increased surface energy, the increased surface roughness and the formation of functional groups on polyimide films after plasma treatment. It appeared that argon and oxygen plasma treatment provide higher surface energy, thereby leading to improved adhesion. Also, surface roughness increases the surface area and provides the physical interactions and mechanical interlocking with metal layer. However, the excessive treatment of polyimide films leads to the formation of weak boundary layer between metal and polyimide. Analysis of FTIR from argon plasma treated polyimide films showed the increased C=O, C-O-C functional groups, which provide stronger chemical bonding with metal layer, at duration of 1 minute. The number of functional groups decreases with increasing time after one minute treatment. As a result of the characterization, the optimal argon plasma settings such as duration of 1 min, top power of 40W, substrate bias power of 125W, and argon flow rate of 30 sccm are selected. The optimal oxygen plasma settings cannot be determined because the chemical structure analysis of the oxygen plasma treated polyimide surfaces cannot be obtained by FTIR so the chemical analysis of the oxygen treated polyimide surfaces should be investigated by advance characterization techniques such as XPS. The electroplating experiments show that the smooth surface morphology was obtained at a mean current density of 8 mA/cm^2 and 90 ms on period, 10 ms off period. SEM micrographs show that the balanced on and off periods give the smooth, uniform surface morphology. 90 ms on period and 10 ms off period were selected as optimum pulse waveforms. In this study, Ti was selected as a adhesion promoting layer. Different type of metals like Cr or TaN can be used and their effects on the adhesion can be investigated for future work. Different type of additive effects on the film properties can be investigated for future work.

REFERENCES

[1] **Egitto F. D. and Matienzo L. J.,** 1994: Plasma modification of polymer surfaces for adhesion improvement.

[2] **Cho S. H., Kim S. H., Lee N.-E., Kim H. M, and Nam Y. W.,** 2005: Micro-scale metallization on flexible polyimide substrate by Cu electroplating using SU-8 photoresist mask, *Thin Solid Films* **475**, 68-71.

[3] **Kim K., Lee K. R., Kim W. H., Park K.-B., Kim T.-H., Kim J.-S., and Pak J. J.,** 2009: Polymer-based flexible tactile sensor up to 32x32arrays integrated with interconnection terminals, *Sensors and Actuators A: Physical* **156**, 284-291.

[4] **Ramos M. M. D.,** 2002: Theoretical study of metal-polyimide interfacial properties, *Vacuum* **64**, 255-260.

[5] **Lin Y.-S. and Liu H.-M.,** 2008: Enhanced adhesion of plasma-sputtered copper films on polyimide substrates by oxygen glow discharge for microelectronics, *Thin Solid Films* **516**, 1773-1780.

[6] **Kim S. H., Na S. W., Lee N.-E., Nam Y. W., and Kim Y.-H.,** 2005: Effect of surface roughness on the adhesion properties of Cu/Cr films on polyimide substrate treated by inductively coupled oxygen plasma, *Surface and Coatings Technology* **200**, 2072-2079.

[7] **Lin Y.-S., Liu H.-M., and Tsai C.-W.,** 2005: Nitrogen plasma modification on polyimide films for copper metallization on microelectronic flex substrates, *J. Polym. Sci. B Polym. Phys.* **43**, 2023-2038.

[8] **Cho S. H., Kim S. H., Lee J. G., and Lee N.-E.,** 2005: Micro-scale metallization of high aspect-ratio Cu and Au lines on flexible polyimide substrate by electroplating using SU-8 photoresist mask, *Microelectronic Engineering* **77**, 116-124.

[9] **Yang C.-hao, Lee S.-chin, Wu J.-ming, and Lin T.-chai,** 2005: The properties of copper films deposited on polyimide by nitrogen and oxygen plasma pre-treatment, *Applied Surface Science* **252**, 1818-1825.

[10] **Lin Y.-S., Liu H.-M., and Chen H.-T.,** 2006: Surface modification of polyimide films by argon plasma for copper metallization on microelectronic flex substrates, *J. Appl. Polym. Sci.* **99**, 744-755.

[11] **Choukourov A., Hanus J., Kousal J., Grinevich A., Pihosh Y., Slavinski D., and Biederman H.,** 2006: Plasma polymer films from sputtered polyimide, *Vacuum* **81**, 517-526.

[12] **Park S.-J. and Lee H.-Y.,** 2005: Effect of atmospheric-pressure plasma on adhesion characteristics of polyimide film, *Journal of Colloid and Interface Science* **285**, 267-272.

[13] **Pappas D. L., Cuomo J. J., and Sachdev K. G.,** 1991: Studies of adhesion of metal films to polyimide.

[14] **Ektessabi A. M. and Hakamata S.,** 2000: XPS study of ion beam modified polyimide films, *Thin Solid Films* **377-378**, 621-625.

[15] **Park S. C., Yoon S. S., and Nam J. D.,** 2008. Surface characteristics and adhesive strengths of metal on O_2 ion beam treated polyimide substrate, *Thin Solid Films* **516**, 3028-3035.

[16] **Inagaki N., Tasaka S., and Masumoto M.,** 1996: Improved Adhesion between Kapton Film and Copper Metal by Plasma Graft Polymerization of Vinylimidazole, *Macromolecules* **29**, 1642-1648.

[17] **Noh B.-I., Yoon J.-W., andJung S.-B.,** 2011: Fabrication and adhesion strength of Cu/Ni-Cr/polyimide films for flexible printed circuits, *Microelectronic Engineering* **88**, 1024-1027.

[18] **Woytasik M., Grandchamp J.-P., Dufour-Gergam E., Gilles J.-P., Megherbi S., Martincic E., Mathias H., and Crozat P.,** 2006: Two- and three-dimensional microcoil fabrication process for three-axis magnetic sensors on flexible substrates, *Sensors and Actuators A: Physical* **132**, 2-7.

[19] **Park B.-N., Bae S.-C., Son S.-H.,. Lee J.-H, and Choi S.-Y.,** 2001: Film Properties of Copper Grown by the Electroplating Process, *Journal of the Korean Physical Society* **38**, 232-235.

[20] **Ruythooren W., Attenborough K., Beerten S., Merken P., Fransaer J., Beyne E., Van Hoof C., De Boeck J., and Celis J. P.,** 2000: Electrodeposition for the synthesis of Microsystems, *J. Micromech. Microeng.*, 101-107.

[21] **Quemper J.-M., Gergam E. D., Rodriguez N. F., Gilles J.-P., Grandchamp J.-P., and Bosseboeuf A.,** 2000: Effects of direct and pulse current on copper electrodeposition through photoresist molds, *Journal of Micromechanics and Microengineering* **10**.

[22] **Watanabe T.,** 2004: Database for the Microstructure of Plated Films, in *Nano Plating - Microstructure Formation Theory of Plated Films and a Database of Plated Films*, pp. 255-696, Elsevier, Oxford.

[23] **Ghariehali A. T. K.,** 2008: Fabrication of high-aspect-ratio metallic micro-structures by reverse exposure method, National University of Singapore.

[24] **Seah C. H., Mridha S., and Chan L. H.,** 2001: DC/pulse plating of copper for trench/via filling, *Journal of Materials Processing Technology* **114**, 233-239.

[25] **Fujita T., Nakamichi S., Ioku S., Maenaka K., and Takayama Y.,** 2007: Seedlayer-less gold electroplating on silicon surface for MEMS applications, *Sensors and Actuators A: Physical* **135**, 50-57.

[26] **Chandrasekar M. S. and Pushpavanam M.,** 2008: Pulse and pulse reverse plating--Conceptual, advantages and applications, *Electrochimica Acta* **53**, 3313-3322.

[27] **Zinsou M.,** 2008: Development and optimization of pulse plating of copper films for MEMS applications, *NNIN REU Research Accomplishments*, 148-149.

[28] **Bu W., Yin J., Tian F., Li G., and Lei Q.,** Effect of corona ageing on the structure changes of polyimide and polyimide/Al2O3 nanocomposite films, *Journal of Electrostatics* **In Press, Corrected Proof**.

[29] J**inghe Z., Mingyan Z., Qibin J., Shujin Z., Tiequan D., Binfen C., and Qingquan L.,** 2006: Synthesis and characterization of silica-alumina co-doped polyimide film, *Materials Letters* **60**, 585-588.

[30] **Maggioni G., Carturan S., Boscarino D., Mea G. D., and Pieri U.,** 1997: Polyimide and platinum containing polyimide thin films obtained by vapour deposition polymerization; effects of thermal treatments, *Materials Letters* **32**, 147-150.

[31] **Ürgen M. and Kazmanlı K.,** 2009: Modern surface modification techniques lecture notes.

CURRICULUM VITAE

Candidate's full name:	Meryem Öznur Pehlivaner
Place and date of birth:	Kırşehir, 17.03.1986
Permanent Address:	Caferağa mah. Dr. Esat Işık cad. Pınar apt. 76/12 Moda-Kadıköy/ İSTANBUL
Universities and Colleges attended:	B.Sc. (2004-2009), ITU, Textile Engineering

Publications:

- **Uçar N., Demir A., Pehlivaner Ö., Onbaşı Ç., Şen B., Koç O.,** "Water Vapor Absorption Performance Of A Novel Composite Fiber", Tekstil ve Konfeksiyon, 1/2010, 4-8.